

12

POLY EE/EP 76-022  
NOVEMBER 1976

# HEAT-PIPE BISMUTH VAPOR LASER;

EXAMINATION OF LASER ACTION AT 4722Å BISMUTH VAPOR

BY WILLIAM T. WALTER AND NICHOLAS SOLIMENE

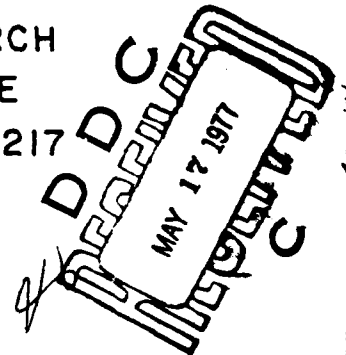
AD A 039568

CONTRACT No. N00014-67-A-0438-0015  
FINAL TECHNICAL REPORT

PERIOD COVERED:  
1 MAY 1973 TO 31 JANUARY 1975

PREPARED FOR:

OFFICE OF NAVAL RESEARCH  
PHYSICS PROGRAM OFFICE  
ARLINGTON, VIRGINIA 22217



APPROVED FOR PUBLIC RELEASE; DISTRIBUTION IS UNLIMITED.  
REPRODUCTION IN WHOLE OR IN PART IS PERMITTED FOR ANY  
PURPOSE OF THE UNITED STATES GOVERNMENT.

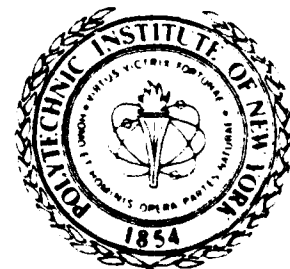
Department of  
Electrical Engineering  
and Electrophysics

DDC FILE COPY

## Polytechnic

Polytechnic Institute of New York

New York City: 333 Jay Street, Brooklyn, New York 11201  
Long Island: Route 110, Farmingdale, New York 11735



UNCLASSIFIED

SECURITY CLASSIFICATION OF THIS PAGE (When Data Entered)

REPORT DOCUMENTATION PAGE		READ INSTRUCTIONS BEFORE COMPLETING FORM
1. REPORT NUMBER	2. GOVT ACCESSION NO.	3. RECIPIENT'S CATALOG NUMBER
4. TITLE (and Subtitle) HEAT-PIPE BISMUTH LASER; Examination of laser action at 4722Å in bismuth vapor.		5. TYPE OF REPORT & PERIOD COVERED Final Report. 1 May 1973-31 Jan. 1975
7. AUTHOR(s) William T. / Walter and Nicholas / Solimene		6. PERFORMING ORG. REPORT NUMBER POLY-EE/EP-76-022
8. PERFORMING ORGANIZATION NAME AND ADDRESS Polytechnic Institute of New York Route 110 Farmingdale, New York 11735		9. CONTRACT OR GRANT NUMBER(s) N00014-67-A-0438-0015
10. CONTROLLING OFFICE NAME AND ADDRESS Office of Naval Research Physics Program Office, Arlington, Va. 22217		11. PROGRAM ELEMENT, PROJECT, TASK AREA & WORK UNIT NUMBERS 12. REPORT DATE Nov 1976
13. MONITORING AGENCY NAME & ADDRESS (if different from Controlling Office) Office of Naval Research Resident Representative 715 Broadway New York, New York 10003		14. NUMBER OF PAGES 59
15. DISTRIBUTION STATEMENT (of this Report) Approved for public release; distribution is unlimited.		16. SECURITY CLASS. (of this report) UNCLASSIFIED
17. DISTRIBUTION STATEMENT (of the abstract entered in Block 20, if different from Report)		18. DECLASSIFICATION/DOWNGRADING SCHEDULE
19. SUPPLEMENTARY NOTES		
20. KEY WORDS (Continue on reverse side if necessary and identify by block number) metal vapor lasers pulsed gas-discharge lasers efficient, visible lasers bismuth vapor pressure and composition bismuth dimers heat-pipe, bismuth working fluid transition probabilities, bismuth computer modeling, laser kinetics excitation cross sections		
21. ABSTRACT (Continue on reverse side if necessary and identify by block number) The possibility of producing efficient pulsed laser action at 4722Å in the neutral atomic vapor of bismuth has been examined. The presence of a substantial fraction of dimers (Bi <sub>2</sub> molecules) in the vapor of bismuth could prevent laser action by absorption of the 3067Å Bi resonance line. This would not only reduce radiation trapping but would also produce dissociation of the		

DD FORM 1473

EDITION OF 1 NOV 68 IS OBSOLETE  
S/N 0102-LF-014-6601

UNCLASSIFIED

SECURITY CLASSIFICATION OF THIS PAGE (When Data Entered)

UNCLASSIFIED

SECURITY CLASSIFICATION OF THIS PAGE (When Data Entered)

20.

dimers leaving one Bi atom in the  $6p^3 2D_{3/2}^0$  metastable proposed lower laser level. Heat pipes were used to create a two temperature zone apparatus and thermally dissociate bismuth dimers. Double-pulses were used to produce discharge dissociation of bismuth dimers. The pressure and composition of bismuth vapor has been critically evaluated. A radial discharge was used to reduce the risetime of the excitation current pulse to  $25 \text{ nsec}$  which is much shorter than the reciprocal of  $5.3 \times 10^6 / \text{sec}$ , the best value for the  $4722\text{\AA}$  transition probability. We conclude that the following three explanations cannot account for the absence of laser action at  $4722\text{\AA}$ : (1) insufficiently fast risetime of the excitation current pulse, (2) the presence of dimers in the vapor or (3) unfavorable ratio of electron excitation cross sections for the  $6p^2 7s^4 P_{1/2}$  resonance and  $6p^3 2D_{3/2}$  metastable levels. The most likely explanation is competing processes within the bismuth atom. In particular we conclude that the Corliss-Bozman value of the  $6p^2 7s^4 P_{3/2} \rightarrow 6p^3 4S_{3/2}$  transition probability is at least a factor of 20 too low. Continuation of the computer modeling begun in this study could verify whether excitation of the  $6p^2 7s^4 P_{3/2, 5/2}$  levels are the competing excitation channels which prevent laser action by strong spontaneous emission to the  $6p^3 2D_{3/2}$  metastable level. Additional computer modeling will also be important in the evaluation of other atomic vapor systems as efficient, high-power lasers.

UNCLASSIFIED

SECURITY CLASSIFICATION OF THIS PAGE (When Data Entered)

HEAT-PIPE BISMUTH VAPOR LASER;  
Examination of laser action at  $4722\text{\AA}$  in bismuth vapor

by  
WILLIAM T. WALTER and NICHOLAS SOLIMENE  
POLYTECHNIC INSTITUTE OF NEW YORK  
ROUTE 110  
FARMINGDALE, NEW YORK 11735

NOVEMBER 1976

FINAL TECHNICAL REPORT  
CONTRACT N00014-67-A-0438-0015  
FOR THE PERIOD 1 May 1973 to 31 Jan. 1975

Sponsored by

OFFICE OF NAVAL RESEARCH  
PHYSICS PROGRAM OFFICE  
ARLINGTON, VIRGINIA 22217

YES	Write Section	<input checked="" type="checkbox"/>
NO	Write Section	<input type="checkbox"/>
UNANNOUNCED		<input type="checkbox"/>
JUSTIFICATION		
BY		
DISTRIBUTION/AVAILABILITY CODES		
Dist.	AVAIL. ORG. OR SPECIAL	
A		

Approved for public release; distribution is unlimited.

Reproduction in whole or in part is permitted for any  
purpose of the United States Government.

## ABSTRACT

The possibility of producing efficient pulsed laser action at  $4722\text{\AA}$  in the neutral atomic vapor of bismuth has been examined. The presence of a substantial fraction of dimers ( $\text{Bi}_2$  molecules) in the vapor of bismuth could prevent laser action by absorption of the  $3067\text{\AA}$  Bi resonance line. This would not only reduce radiation trapping but would also produce dissociation of the dimers leaving one Bi atom in the  $6p^3\ ^2D_{3/2}^0$  metastable proposed lower laser level. Heat pipes were used to create a two-temperature zone apparatus and thermally dissociate bismuth dimers. Double-pulses were used to produce discharge dissociation of bismuth dimers. The pressure and composition of bismuth vapor has been critically evaluated. A radial discharge was used to reduce the risetime of the excitation current pulse to  $\sim 25$  nsec which is much shorter than the reciprocal of  $5.3 \times 10^6 \text{ sec}^{-1}$ , the best value for the  $4722\text{\AA}$  transition probability. We conclude that the following three explanations cannot account for the absence of laser action at  $4722\text{\AA}$ : (1) insufficiently fast risetime of the excitation current pulse, (2) the presence of dimers in the vapor or (3) unfavorable ratio of electron excitation cross sections for the  $6p^2\ 7s\ ^4P_{1/2}$  resonance and  $6p^3\ ^2D_{3/2}$  metastable levels. The most likely explanation is competing processes within the bismuth atom. In particular we conclude that the Corliss-Bozman value of the  $6p^2\ 7s\ ^4P_{3/2} \rightarrow 6p^3\ ^4S_{3/2}$  transition probability is at least a factor of 20 too low. Continuation of the computer modeling begun in this study could verify whether excitation of the  $6p^2\ 7s\ ^4P_{3/2, 5/2}$  levels are the competing excitation channels which prevent laser action by strong spontaneous emission to the  $6p^3\ ^2D_{3/2}$  metastable level. Additional computer modeling will also be important in the evaluation of other atomic vapor systems as efficient, high-power lasers.

## ACKNOWLEDGEMENT

This report was prepared as a comprehensive examination of the possibility of laser action at  $4722\text{\AA}$  in bismuth vapor. The experimental investigation of the generation of laser action by the dissociation of bismuth dimers in the vapor was carried out under this ONR Contract. Additional work to identify the mechanism responsible for the absence of laser action was supported in part by ARPA under ONR Contract N00014-67-A-0438-0017 and in part under the Joint Services Electronics Program under AFOSR Contract F44620-74-C-0056.

## TABLE OF CONTENTS

Abstract	i
Acknowledgement	ii
Table of Contents	iii
List of Illustrations	iv
List of Tables	vi
1. Introduction	1
2. Risetime of the Excitation Current Pulse	4
3. Transition Probability of the $4722\text{\AA}^0$ Line	6
4. Bismuth Vapor Pressure and Composition	10
5. The Effect of Dimers in Bismuth Vapor	14
6. Thermal Dissociation of Bismuth Dimers	18
7. Discharge Dissociation of Bismuth Dimers	21
8. Competing Processes	26
9. Computer Modeling	28
10. Electron Excitation Cross Sections of the Proposed Bismuth Laser Levels	31
11. Electron Collisional Mixing Between Laser Levels	35
12. A Possible Explanation for the Absence of Laser Action	35
13. Modeling of the Initial Breakdown Process	42
14. Summary and Conclusions	43
15. References	
Appendix I - Improved Values of Atomic Transition Probabilities	
Appendix II - Computer Modeling of the Dynamics of Metal Vapor Lasers	

## LIST OF ILLUSTRATIONS

<u>Figure</u>		<u>Page</u>
1.	Efficient pulsed gas-discharge laser in an atomic vapor.	2
2.	Proposed pulsed laser transition at $4722\text{\AA}$ in bismuth vapor indicated on a partial energy level diagram of bismuth	3
3.	Composition of bismuth vapor - the percentage of dimers in the vapor as a function of the total equilibrium vapor pressure of bismuth	11
4.	Total equilibrium vapor pressure of bismuth as a function of the reciprocal of the absolute temperature	12
5.	Comparison of the mole fraction of dimers in the vapors of bismuth, copper and lead	15
6.	Split heat-pipe apparatus to establish two distinct temperature zones in the furnace	19
7.	Hot-window quartz-tube laser-discharge apparatus capable of sustained operation at temperatures up to $1000^{\circ}\text{C}$ for copper halide and bismuth dimer vapors	22
8.	Double-pulse excitation system for copper halide and bismuth dimer vapors	23
9.	Comparison of the situation in bismuth with that in copper for a) expected pulsed laser action, b) oscillator strengths (f values) out of the ground levels and c) radiative filling (A values) of the proposed, metastable, lower laser levels	27
10.	Computer modeling of a pulsed discharge in bismuth vapor where the capacitor voltage (V), discharge tube current density (I) and expected $4722\text{\AA}$ laser output (*) are shown as a function of time. Gryzinski cross sections are used.	30



## LIST OF ILLUSTRATIONS (continued)

<u>Figure</u>		<u>Page</u>
11.	Computer modeling of a pulsed discharge in bismuth vapor where the capacitor voltage (V), discharge tube current density (I) and expected $4722\text{\AA}$ laser output (*) are shown as a function of time Gryzinski cross sections have been normalized to WTB values at 40eV.	32
12.	Electron collisional mixing between laser levels has been added to the computer modeling shown in Fig. 11.	36
13.	Energy loss spectrum for 40eV electrons incident on a bismuth vapor beam measured by Williams, Trajmar and Bozinis.	40

# LIST OF TABLES

<u>Table</u>		<u>Page</u>
1.	Transition Lifetime for Pulsed Laser Action in Neutral Atomic Vapors	5
2.	Lifetime of $6p^2 7s^4 P_{1/2}$ Bismuth Resonance Level	8
3.	Branching Ratio into the $4722\text{\AA}^0$ Bismuth Transition	9
4.	Thermal Dissociation of Bismuth Dimers in the Split Heat-Pipe Apparatus of Fig. 6	20
5.	Comparison of Integral Electron Excitation Cross Sections (in units of $10^{-16}\text{cm}^2$ ) for the Upper and Lower Laser Levels in Atomic Copper, Lead and Bismuth	34
6.	Comparison of Line Strengths for the Resonance Multiplets of Arsenic, Antimony and Bismuth	38
7.	Comparison of Spontaneous Radiation Rates into the $2D_{3/2}$ Proposed Lower Laser Level from the $4P_{1/2, 3/2, 5/2}$ Resonance Levels.	41

## 1. INTRODUCTION

For efficient, high-power lasers with a visible or ultraviolet output, Walter, Solimene, Piltch and Gould<sup>1</sup> proposed a class of pulsed, gas discharge lasers in neutral atomic vapors. Pulsed electron excitation of the resonance levels of certain atoms with suitable, low-lying energy level structures can efficiently produce pulsed laser action to a metastable level lying between the ground level and the resonance level as indicated in Fig. 1. This type of pulsed laser action has been demonstrated in the vapors of Pb<sup>2</sup>, Mn<sup>3</sup>, Cu<sup>4</sup>, Au<sup>5</sup>, Ca<sup>6</sup>, Sr<sup>6</sup> and Ba<sup>7</sup>. Most experimental effort has been applied to the copper vapor laser. Peak powers of 170 kW and average powers of 15 W have been generated at 5105 Å in copper vapor with a 1% overall electrical efficiency<sup>8</sup>.

Similar laser action is possible in other elements as indicated in Table IV of Reference 1. One of the most interesting possibilities is that in bismuth where laser action should occur at 4722 Å as indicated in Fig. 2. This wavelength is close to the wavelength of maximum transmission through water, so development of an efficient, high-power pulsed bismuth laser would be useful for a number of naval applications. However, in spite of attempts in a number of different laboratories, laser action has not, to our knowledge, been observed at 4722 Å in the vapor of bismuth.

Four possible explanations for the absence of laser action at 4722 Å in pulsed discharges in bismuth vapor are:

- (1) insufficiently fast risetime of the excitation current pulse,
- (2) the presence of dimers, Bi<sub>2</sub>, in the vapor,
- (3) unfavorable ratio of electron excitation cross sections for the resonance and metastable levels, and
- (4) competing processes; such as, excitation to levels other than the resonance level and cascade filling of the metastable, proposed lower laser level.

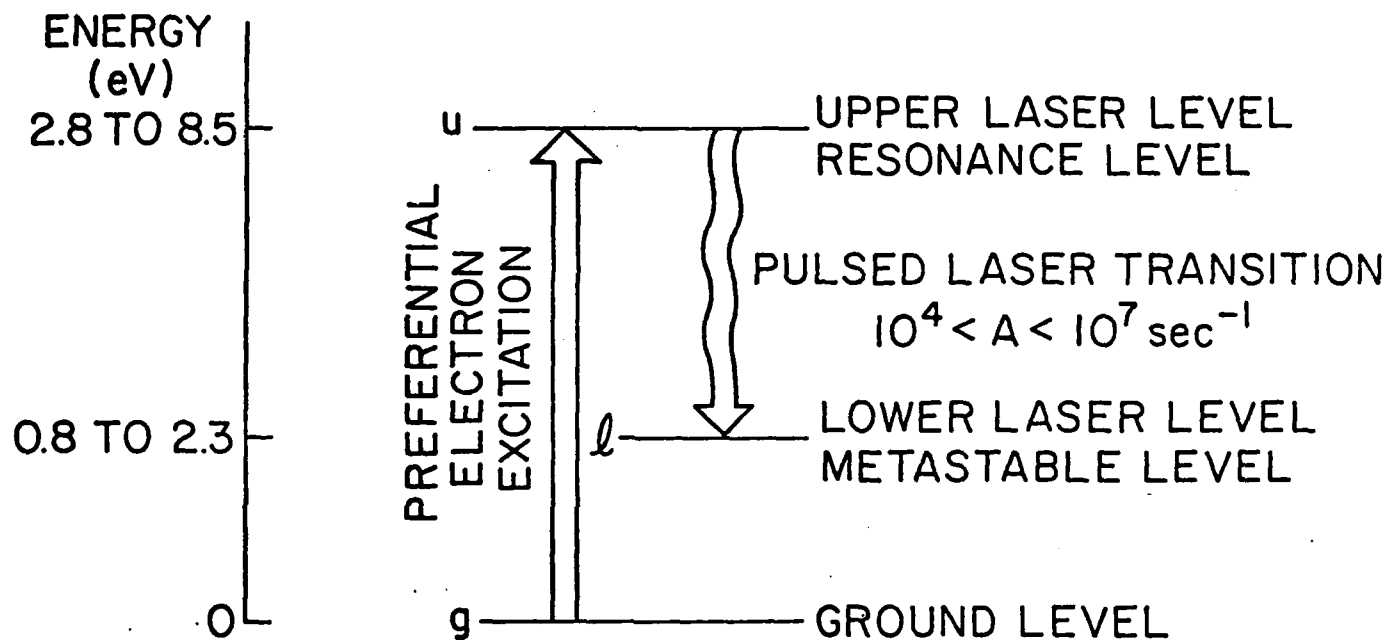


Fig. 1 Efficient pulsed gas-discharge laser  
in an atomic vapor.

# BISMUTH

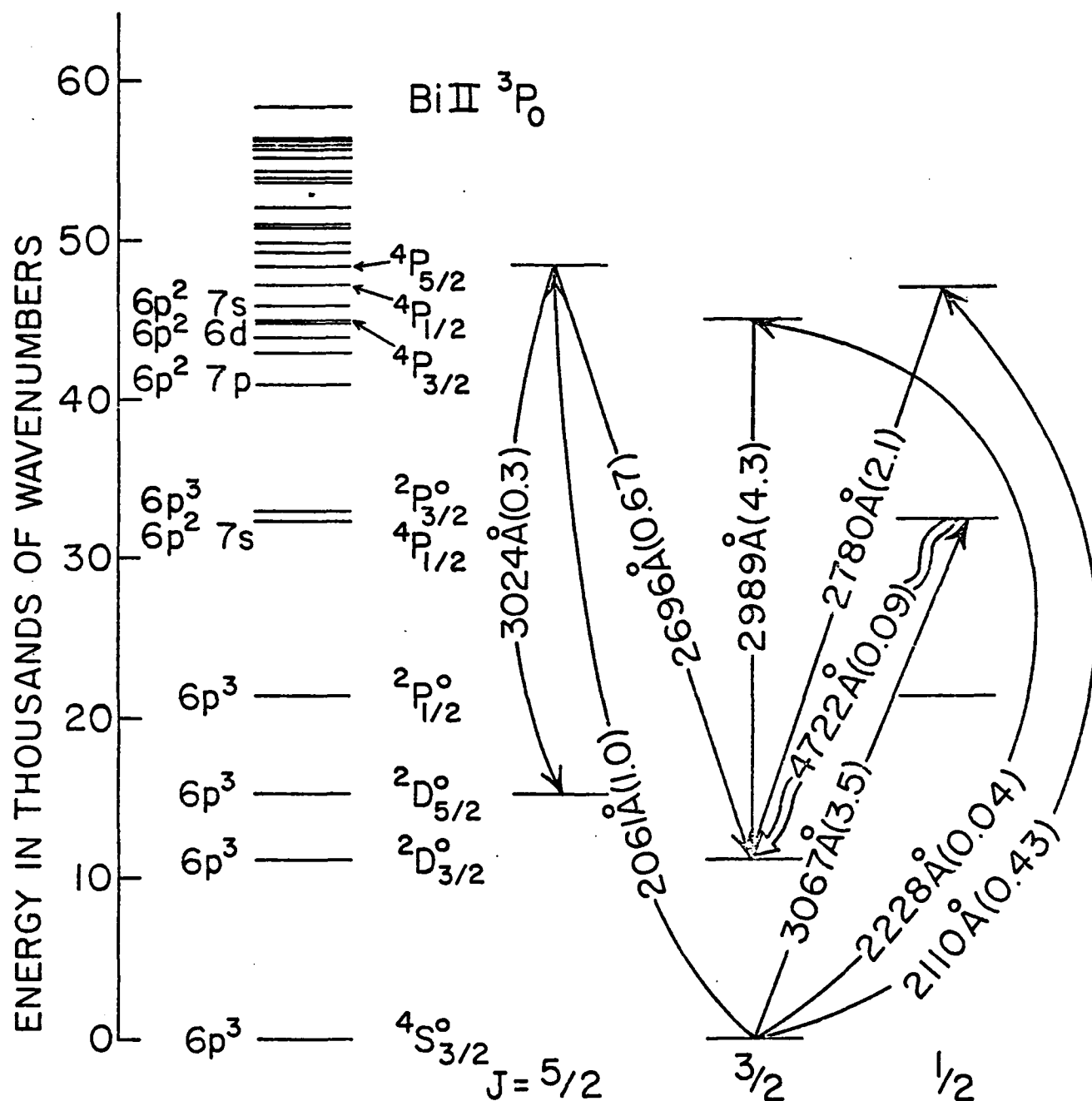


Fig. 2 Proposed pulsed laser transition at  $4722\text{\AA}$  in bismuth vapor indicated on a partial energy level diagram of bismuth. Figures in parentheses are Corliss-Bozman<sup>10</sup> transition probabilities in units of  $10^8 \text{ sec}^{-1}$ .

Each of these possible explanations for the lack of laser action in bismuth vapor was examined during this study. The experimental risetime of the excitation current pulse was reduced to  $\sim 25$  nsec to overcome the limitation of (1). Two different methods were used to dissociate the bismuth dimers and remove limitation (2). A computer model of the kinetics of the excitation and relaxation processes was employed to examine the electron excitation rates (3) and the competing processes (4) in a bismuth vapor discharge. In the following sections of this report, each of these approaches will be separately discussed and assessed.

## 2. RISETIME OF THE EXCITATION CURRENT PULSE

One of the criteria for efficient, pulsed atomic-vapor lasers<sup>1</sup> is that the risetime of the excitation current pulse must be faster than the reciprocal of the transition probability,  $A_{ul}$ , of the proposed laser line for laser action to be achieved in a three level energy level structure as indicated in Fig. 1. If this criterion is not satisfied, spontaneous radiation will drain the upper laser level and fill the metastable lower laser level, thereby preventing the establishment of a population inversion. The total upper level lifetime  $(A_{ul} + A_{ug})^{-1} \approx A_{ul}^{-1}$ , because the resonance radiation is well trapped at the operating temperature for pulsed laser action. For example, in a 1 cm diam tube at 1100°K containing 0.1 torr of atomic bismuth vapor pressure, the radiation-trapped transition probability<sup>9</sup> of the 3067Å resonance line has been reduced from  $2 \times 10^8$  to  $1 \times 10^5 \text{ sec}^{-1}$ ; and the atomic bismuth vapor pressure for optimum peak laser power is expected to be  $> 0.1$  torr.

Table 1 lists the transition lifetimes for pulsed laser lines which have previously been observed in our metal vapor facilities. According to Corliss and Bozman<sup>10</sup> the 4722Å bismuth transition lifetime is 111 nsec. Excitation pulse risetimes in our various metal vapor discharge tubes have been 50 to 100 nsec. Since we have observed laser action on the Mn 1.29μ transition with an upper level lifetime similar to the Bi 4722Å transition, and we have

TABLE 1  
Transition Lifetimes for Pulsed Laser Action  
in Neutral Atomic Vapors

Transition [Å]		Classification	$[10^8 \text{A}^{\text{a}} \text{sec}^{-1}]$	$\tau=1/\text{A}$ [nsec]	Laser Action
Cu	5105.5	$4p^2 \text{P}^{\circ}_{3/2} \rightarrow 4s^2 \text{D}_{5/2}$	.013	770	observed
Pb	7229.0	$7s^3 \text{P}^{\circ}_1 \rightarrow 6p^2 \text{D}_2$	.022	450	observed
Au	6278.1	$6p^2 \text{P}^{\circ}_{1/2} \rightarrow 6s^2 \text{D}_{3/2}$	.024	420	observed
Cu	5782.1	$4p^2 \text{P}^{\circ}_{1/2} \rightarrow 4s^2 \text{D}_{3/2}$	.027	370	observed
Mn	5341.0	$y^6 \text{P}^{\circ}_{7/2} \rightarrow a^6 \text{D}_{9/2}$	.033	300	observed
Mn	12899.8	$z^6 \text{P}^{\circ}_{7/2} \rightarrow a^6 \text{D}_{9/2}$	.081 <sup>b</sup>	123	observed
Bi	4722.1	$7s^4 \text{P}_{1/2} \rightarrow 6p^2 \text{D}^{\circ}_{3/2}$	.090	111	not observed
Pb	4062.1	$6d^3 \text{D}^{\circ}_1 \rightarrow 6p^2 \text{D}_2$	1.07	9	observed

a Corliss and Bozman, Reference 10.

b Calculated, Piltch et al., Reference 3, based on the Corliss-Bozman value for the 5341 Å Mn transition.

observed laser action on the Pb 4062 Å nm transition with a shorter lifetime; it seems unlikely that insufficiently fast pulse risetime is the cause for the lack of success in busmuth.

Furthermore, during the course of this investigation we have improved the electrical discharge circuit - producing a radial discharge between a wire at the center and a cylindrical electrode at the wall of the discharge tube. This configuration reduced the risetime of the current pulse to ~ 25 nsec. Still no laser action was observed in the bismuth vapor discharge.

### 3. TRANSITION PROBABILITY OF THE 4722 Å<sup>0</sup> BISMUTH LINE

In the comparison of excitation risetime with the transition lifetime, the possibility of a significant error in the Corliss-Bozman value of the transition probability should also be considered. Transition probabilities of some 25,000 classified lines in 70 elements have been calculated by Corliss and Bozman<sup>10</sup> from the intensity tables of Meggers, Corliss and Scribner<sup>11</sup>. The Corliss-Bozman transition probabilities are particularly useful for examination and comparison of potential pulsed laser action in a large number of elements; however, substantial errors have been reported in a number of these values, some as large as a factor of 20. Therefore, one is reluctant to rely very strongly on these values.

Accurate values of atomic transition probabilities are most important in the evaluation of new, efficient pulsed-laser systems in other atomic vapors. Because the Corliss-Bozman values<sup>10</sup> remain the only consistent set of transition probabilities spanning the stronger spectral lines of most of the solid elements, we have explored the possibility of improving the Corliss-Bozman values as part of our metal screening program. A procedure has been developed to obtain improved transition probabilities from the spectral line in-



tensities of the Meggers-Corliss-Scribner arc<sup>11</sup> which is described in Appendix I. When Fig. 1 of Appendix I is used with the bismuth parameters ( $E_u = 32588 \text{ cm}^{-1}$ ,  $I = 60 \times 10^3$ ,  $\lambda = 4722 \text{ \AA}$  and  $U = 4.3$ ), an improved Corliss-Bozman transition lifetime of 140 nsec is calculated for the  $4722 \text{ \AA}$  line.

Although apparently no other direct measurements have been carried out on the  $4722 \text{ \AA}$  bismuth line, a number of measurements have been made on the  $3067 \text{ \AA}$  resonance line and of the lifetime of the  $6p^2 7s \text{ } ^4P_{1/2}$  resonance level which is the proposed upper laser level. These measurements, which are compared in Table 2, can be used with the branching ratio to obtain a better value for the transition lifetime of the  $4722 \text{ \AA}$  bismuth line.

Table 2 reveals that all of the other experimental measurements of the  $6p^2 7s \text{ } ^4P_{1/2}$  resonance level lifetime are longer than Corliss and Bozman's 2.8 nsec value. The most accurate value is probably Svanberg's Hanle-effect measurement of 4.75 nsec.

Recently intermediate coupling calculations have been carried out for  $6p^2 7s \rightarrow 6p^3$  transitions in bismuth.<sup>17, 18</sup> The calculated lifetime values are listed in the lower part of Table 2. The transition probabilities calculated depend on the local exchange approximation as well as on the dipole length or dipole velocity forms of the transition probability operator since the self-consistent field wavefunctions are not exact. The difference between the dipole length and dipole velocity calculations can be viewed as an indication of the inexactness of the wavefunctions. The calculations indicate that the lifetime of the  $6p^2 7s \text{ } ^4P_{1/2}$  bismuth resonance level is approximately 5 nsec which is consistent with the best experimental values and is substantially longer than the Corliss-Bozman value.

The branching ratio,  $A_{ul} / \sum_{\text{all } j} A_{uj} = A_{ul} \tau_u$ , may be used to obtain a particular transition lifetime from the level lifetime,  $\tau_u$ . The only experi-

TABLE 2  
Lifetime of  $6p^2 7s \ ^4P_{1/2}$  Bismuth Resonance Level

Measurement	Method	Lifetime (nsec)
Corliss and Bozman <sup>10</sup>	Emission	2.8
Lvov <sup>12</sup>	Absorption	$8.9 \pm 1.8^a$
Rice and Ragone <sup>13</sup>	Absorption	$5.3 - 1.7^{+2.3^a}$
Cunningham and Link <sup>14</sup>	Phase Shift	$5.9 \pm 0.2$
Svanberg <sup>15</sup>	Hanle Effect	$4.75 \pm 0.18$
Anderson, et al. <sup>16</sup>	Beam Foil	$4.7 \pm 1.0$

<sup>a</sup> As corrected in Ref. 14 by using the Corliss-Bozman value of 0.97 for the branching ratio into the 3067 $\text{\AA}$  resonance line.

Intermediate Coupling SCF Calculation	Type of Exchange Approximation	Form	Lifetime
Holmgren <sup>17</sup>	Hartree-Slater	Dipole Length Dipole Velocity	5.7 nsec 2.6 nsec
Holmgren <sup>17</sup>	OHFS-Lingren- Rosen	Dipole Length Dipole Velocity	4.1 nsec 7.1 nsec
Kunisz and Migdalek <sup>18</sup>	Lingren		5.7 nsec

mental values available to determine branching ratios in bismuth are from Corliss and Bozman.<sup>10</sup> These ratios, however, should be more accurate than the value for an individual transition probability since effects other than radiation trapping, such as uncertainty in the degree of ionization or non-uniformity of the arc, are expected to be the dominant sources of error and should substantially cancel out in the ratio.

Branching ratios into the  $4722\text{\AA}$  bismuth transition are also available from the intermediate coupling calculations.<sup>17, 18</sup> These values are in substantial agreement with the Corliss-Bozman value as indicated in Table 3. Using the Corliss-Bozman branching ratio of .025 for the  $4722\text{\AA}$   $4P_{1/2} \rightarrow 2D_{3/2}$  line, we may deduce a 190 nsec transition lifetime from Svanberg's 4.75 nsec  $4P_{1/2}$  level lifetime. This is substantially longer than the 111 nsec Corliss-Bozman value and also longer than our improved value of 140 nsec.

TABLE 3  
Branching Ratio into the  $4722\text{\AA}$  Bismuth Transition

Source	Method	Branching Ratio
Corliss-Bozman <sup>10</sup>	Emission Measurement	0.025
Holmgren <sup>17</sup>	Calculation - OHFS -	
	dipole length	0.020
	dipole velocity	0.047
Kunisz-Migdalek <sup>18</sup>	Calculation	0.026

All indications are, therefore, that the transition lifetime of the  $4722\text{\AA}$  proposed laser transition in bismuth is significantly greater than 100 nsec; the best value being 190 nsec. This corresponds to a spontaneous-emission transition probability for the  $4722\text{\AA}$  bismuth line of  $5.3 \times 10^6 \text{ sec}^{-1}$ . Since excitation risetimes of  $\sim 25$  nsec have been produced and laser action has been obtained on transitions with similar or shorter transition lifetimes in Mn and Pb, it appears to be very unlikely that an insufficiently fast risetime of the current excitation pulse can be the explanation for the absence of laser action at  $4722\text{\AA}$  in bismuth vapor.

#### 4. BISMUTH VAPOR PRESSURE AND COMPOSITION

During the course of this study it became apparent that a serious disagreement exists in the characterization of bismuth vapor as reported in several compilations. A large disparity exists between the most recent compilation of Nesmeyanov<sup>19</sup> and the prior ones of Hultgren et al.<sup>20</sup> and Stull and Sinke.<sup>21</sup> The disparity in dimer percentage is displayed in Fig. 3 by the three solid horizontal lines. The upper line through Hultgren's points<sup>20</sup> indicates a dimer concentration of 50 to 60% in the pressure range of 1 mtorr to 10 torr. The middle line through Nesmeyanov's points<sup>19</sup> indicates a dimer concentration of about 20%, while the lower line through the points of Stull and Sinke<sup>21</sup> indicates a dimer concentration of approximately 10%.

The disparity in total bismuth vapor pressure is shown in Fig. 4. The upper line through Nesmeyanov's points<sup>19</sup> indicates a total bismuth vapor pressure about ten times higher than either the compilation of Hultgren et al.<sup>20</sup> or Stull and Sinke<sup>21</sup> which are represented by the lower line.

To resolve these disparities, the early measurements were reexamined and compared with several recent measurements. On this basis, as described

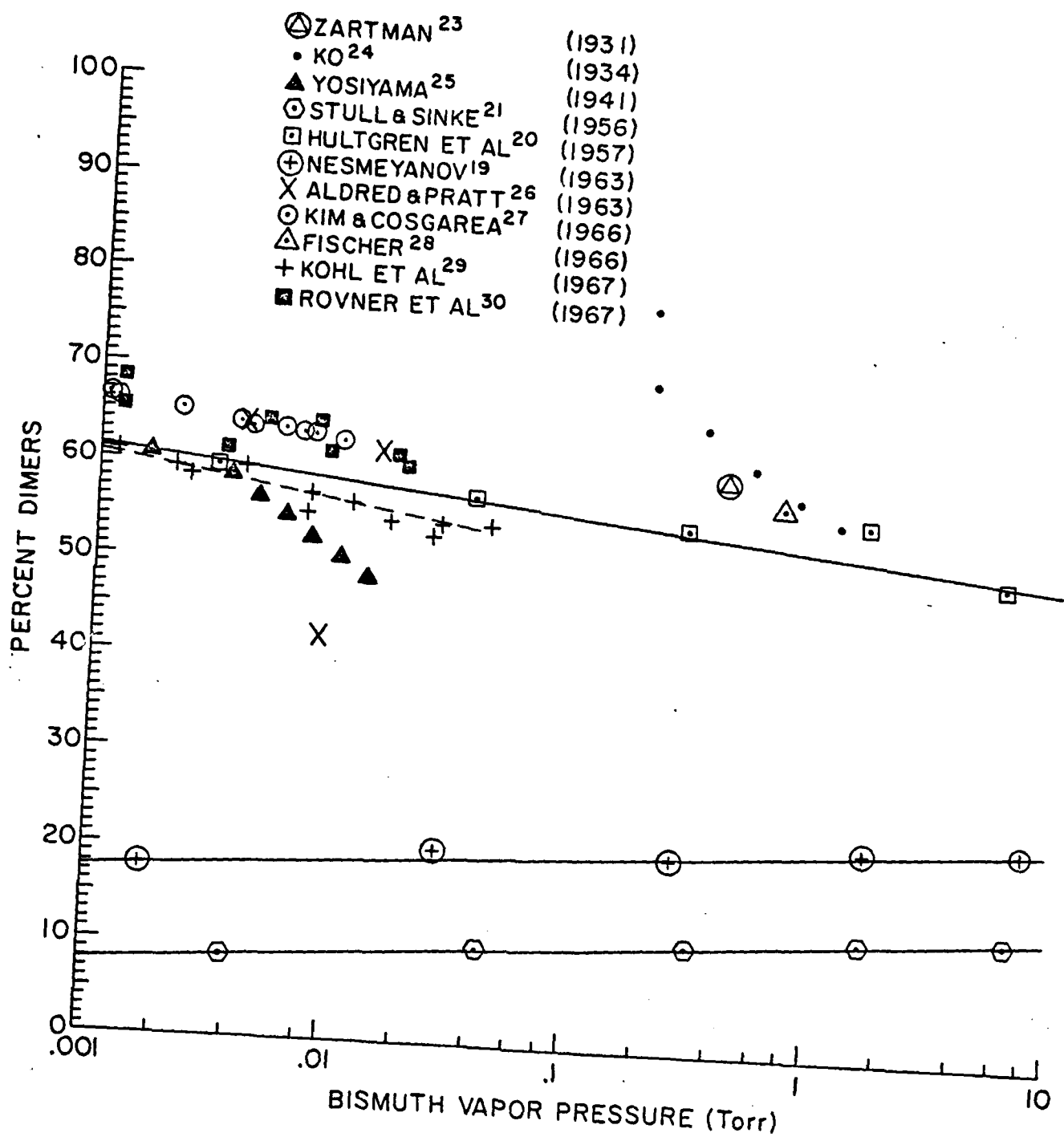


Fig. 3 Composition of bismuth vapor - the percentage of dimers in the vapor as a function of the total equilibrium vapor pressure of bismuth.

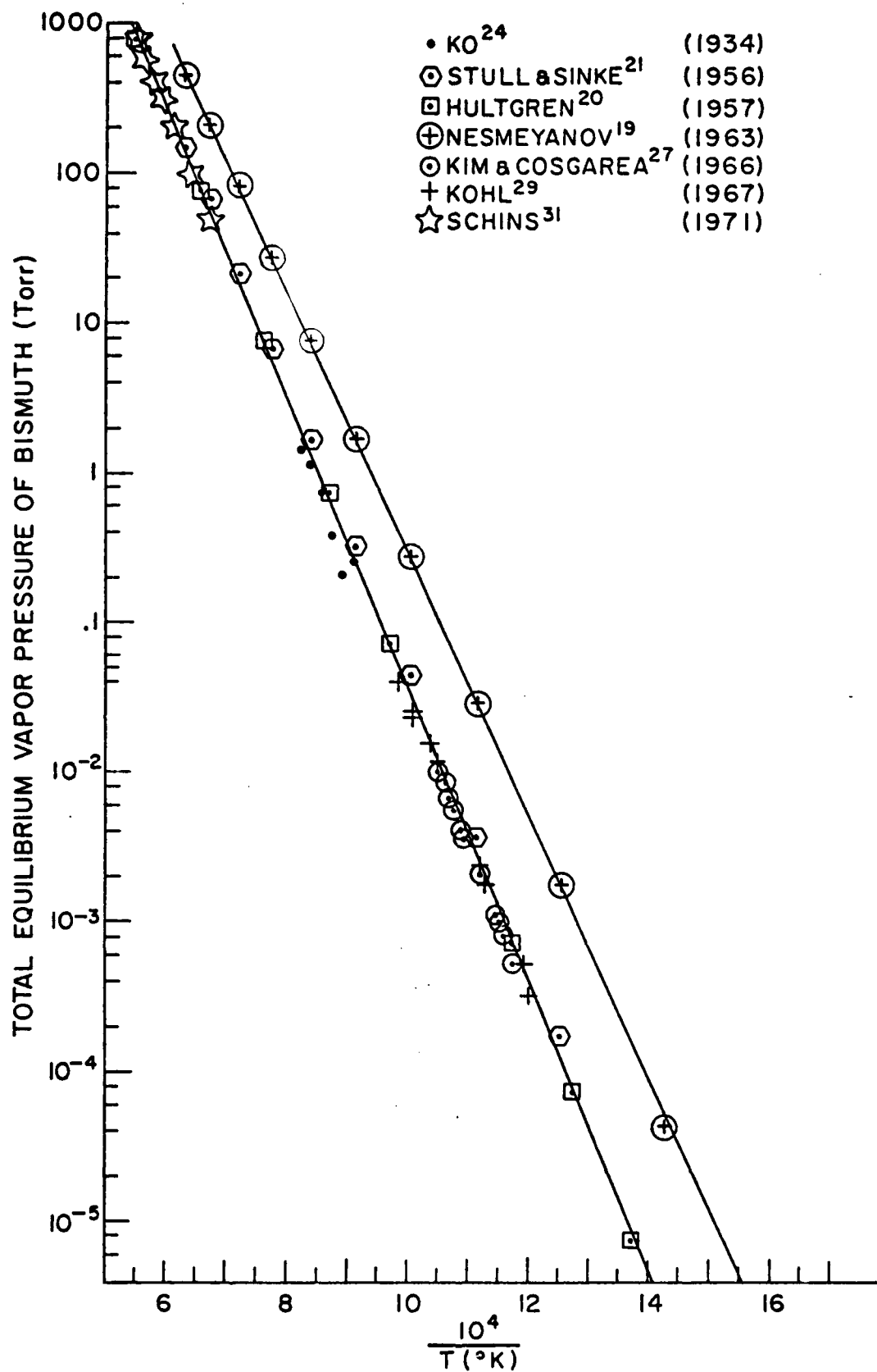


Fig. 4 Total equilibrium vapor pressure of bismuth as a function of the reciprocal of the absolute temperature.

below, we conclude that the compilation of Hultgren et al.<sup>20</sup> best represents the actual situation in bismuth.

In 1928 Leu<sup>22</sup> carried out a Stern-Gerlach experiment using bismuth vapor and in 1931 Zartman<sup>23</sup> used a velocity analyzer on bismuth vapor. Both found that the vapor of bismuth consisted of about 50% Bi<sub>2</sub> molecules at total vapor pressures of 0.1 to 1 torr. Ko<sup>24</sup> corrected and extended these initial experiments and reported dimer concentrations of 60-70% at total vapor pressures of 0.1 to 1 torr. In 1941 Yosiyama<sup>25</sup> using a torsion-effusion method obtained dimer compositions of the bismuth vapor of 40-50% at 1 to 10 mtorr. These experiments, indicating a substantial fraction of dimers in the vapor of bismuth, were not used in the compilations of Nesmeyanov<sup>19</sup> or Stull and Sinke.<sup>21</sup>

More recently the torsion-effusion experiments of Aldred and Pratt<sup>26</sup> and Kim and Cosgarea<sup>27</sup>, the quasi-static and boiling point experiments of Fischer<sup>28</sup> and the mass spectrometric experiments of Kohl, Ul and Carlson<sup>29</sup> and Rovner et al<sup>30</sup> all confirm the earlier work indicating that dimers constitute about half of the vapor of bismuth. These more recent experimental data points are plotted in Fig. 3 along with the earlier measurements. Hultgren's compilation<sup>20</sup> is in reasonable agreement with all of the data in Fig. 3 while the compilations of Nesmeyanov<sup>19</sup> and Stull and Sinke<sup>21</sup> are not and must be rejected. The mass spectroscopic study of Kohl, Ul and Carlson<sup>29</sup> appears to be the most reliable of all the vapor composition experiments. It is in good agreement with the earlier Hultgren compilation within its measurement range (0.3-42 mtorr) as indicated by the dotted line in Fig. 3. This experiment also confirmed the presence of a small amount of Bi<sub>4</sub> molecules (approximately 1%) in this pressure region.

In Fig. 5 where the total bismuth vapor pressure is plotted as a function of the reciprocal of the temperature, data points of the early velocity analyzer measurements of Ko,<sup>24</sup> and the more recent torsion-effusion experiments of Kim and Cosgarea<sup>27</sup> and the mass spectroscopic measurements of Kohl, Ul and Carlson<sup>29</sup> are displayed in addition to points from the three compilations. Also plotted are the recent heat-pipe measurements of Schins et al<sup>31</sup> at high bismuth vapor pressures (>49 torr). All of this data is in substantial agreement with the compilations of Hultgren<sup>20</sup> and Stull and Sinke<sup>21</sup> and in serious disagreement with that of Nesmeyanov.<sup>19</sup>

Our conclusion is that the compilation of Hultgren et al.<sup>20</sup> is the best characterization of both the total bismuth vapor pressure as well as the composition of the vapor in terms of monomers and dimers. Therefore the values of Hultgren have been utilized in this study.

## 5. THE EFFECT OF DIMERS IN BISMUTH VAPOR

The vapor of bismuth contains a substantial percentage of dimers while the vapors of copper and lead do not. Figure 5 compares the dimer concentration in the vapors of bismuth,<sup>20</sup> copper<sup>32</sup> and lead<sup>32</sup> in the pressure range 0.1 mtorr to 100 torr. This is a broader pressure range by a factor of at least ten at each end, than the copper and lead vapor lasers have operated in thus far. The dimer concentration in bismuth vapor is greater than 50% at pressures below 10 torr while the dimer concentration in copper vapor is less than 1% and in lead vapor less than 0.1% in a similar pressure region. At 1 torr of total metallic vapor pressure, for example, where operation of both the copper and lead vapor lasers is very strong, the dimer concentration in bismuth vapor is 53% while it is only 0.4% in copper vapor and 0.06% in the vapor of lead.



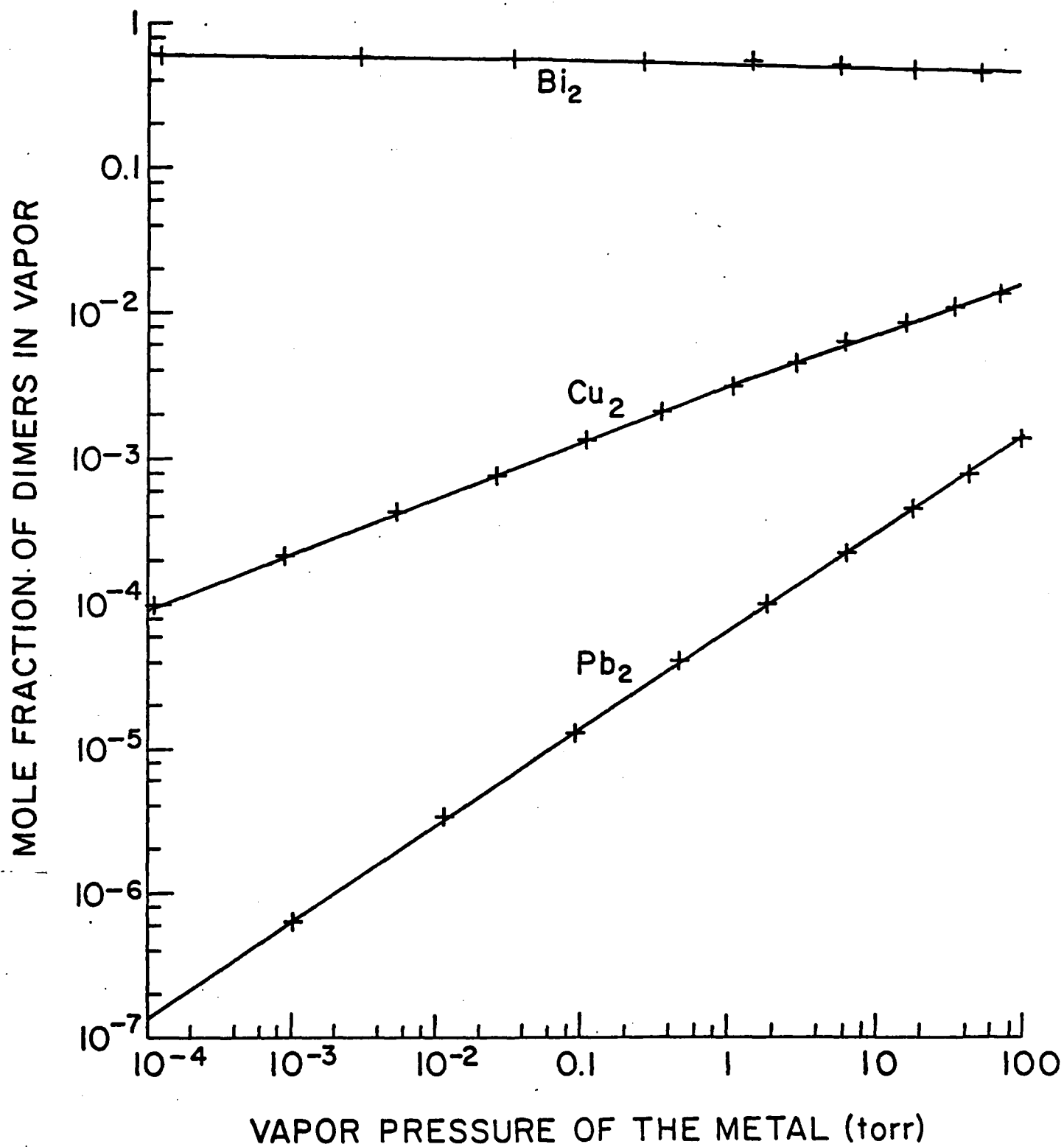


Fig. 5. Comparison of the mole fraction of dimers in the vapors of bismuth, copper and lead.

The presence of bismuth dimers could adversely affect the possibility of laser action at  $4722\text{\AA}$  in several ways:

- (1) directly by absorption at  $4722\text{\AA}$ ,
- (2) by absorption of the  $3067\text{\AA}$  bismuth resonance line which will not only reduce radiation trapping but can produce dissociation of the  $\text{Bi}_2$  dimers leaving one Bi atom in the  $6p^3\ ^2D_{3/2}^o$  meta-stable proposed lower laser level,<sup>33, 34</sup>
- (3) by means of collisional processes which interfere with the excitation process, such as a modification of the electron distribution, or which quench the upper resonance level.

There are at least two possibilities for direct absorption at the proposed laser wavelength by the bismuth dimers. The  $v' = 42 \leftarrow v'' = 9$  band head of the  $A\ \text{O}_u^+ \leftarrow X\ ^1\Sigma_g^+$  absorption band of  $\text{Bi}_2$  is within  $1\text{ cm}^{-1}$  of the  $4722\text{\AA}$  proposed laser transition, and the  $v' = 31 \leftarrow v'' = 2$  band head is only  $8\text{ cm}^{-1}$  below.<sup>33</sup> These absorption bands appear from the literature,<sup>33</sup> however, to be weak. Experimentally, we examined the absorption using a path length of bismuth vapor  $\sim 20\text{cm}$  long and spontaneous emission at  $4722\text{\AA}$  from a second tube of similar length. The temperature of the bismuth in the absorption tube was varied from  $800$  to  $1500^\circ\text{C}$ . To within the measurement accuracy of  $5\%$ , no absorption was measured. Since the gain expected from a  $20\text{ cm}$  path length of this type of pulsed atomic-vapor laser is much greater than  $100\%$ , we conclude that direct absorption by the dimer ground state at  $4722\text{\AA}$  cannot account for the absence of laser action.

Absorption of the  $3067\text{\AA}$  resonance line by the bismuth dimers has just as serious a consequence. Almy and Sparks<sup>33</sup> in their study of the absorption spectrum of bismuth vapor reported a region of continuous absorption which is independent of the other absorption bands they observed. This intense extended continuum appears quite faint at  $900^\circ\text{C}$  with a maximum absorption at  $3120\text{\AA}$ .

At 1000°C it extends roughly from 2950Å to 3350Å, and at 1050°C complete absorption occurs from 2600Å to 3400Å. In their analysis Almy and Sparks<sup>33</sup> accounted for this near ultraviolet continuum with a repulsive level M which dissociates into two bismuth atoms, one in the ground  $^4S_{3/2}$  level but the other in the metastable  $^2D_{3/2}$  level which is the proposed lower laser level. The more recent study of the electronic states of Bi<sub>2</sub> by Gerber and Broida<sup>34</sup> retains the repulsive M level. The deleterious consequences of absorption of the strong atomic bismuth resonance radiation by Bi<sub>2</sub> molecules producing a bismuth atom in the metastable  $^2D_{3/2}$  proposed lower laser level is obvious. This could easily account for the inability to produce laser action at 4722Å in bismuth vapor.

Finally there are also some collisional processes involving the Bi<sub>2</sub> dimers which can affect the generation of a population inversion between atomic bismuth energy levels. In our studies of the effect of additive gases on the power output of the copper vapor laser,<sup>35</sup> the addition of each diatomic or polyatomic gas we have tested has seriously affected the laser's output power. There are two collisional processes by which the additive gas can degrade the laser performance. First there is the possibility of electron-additive gas collisions interfering with the excitation process by lowering the electron temperature. If the additive gas has a low ionization potential and low-lying excited levels compared to those of copper or bismuth; then as the electrons are heated during the excitation process, they can transfer excitation to the additive gas before the electrons acquire enough energy to excite the metal atoms. Low-lying vibration-rotation levels of the additive gas and a low molecular dissociation energy may also contribute to such a parasitic process. The net result can be to keep the electron temperature below the region for

optimum excitation of the copper upper laser levels. A second possibility is that the additive gas molecules may interfere with the excitation process at a somewhat later stage by quenching the copper or bismuth atoms which have already been excited to the upper laser level. Here, additive gas-excited metal atom collisions can transfer the metal atom from the resonance level to either the metastable or ground levels without participating in the laser process. In the case of dimers such as  $\text{Bi}_2$ , the built-in resonance of energy level structures may substantially increase these quenching cross sections.

Therefore at the beginning of this study, the presence of dimers in the vapor of bismuth was considered to be the prime cause for the non-observance of laser action at  $4722\text{\AA}$  in bismuth. We experimentally examined this hypothesis by utilizing two different methods of dissociating the dimers and tested the resulting vapor for laser action: 1) Thermal Dissociation and 2) Discharge Dissociation.

## 6. THERMAL DISSOCIATION OF BISMUTH DIMERS

Heat pipes were used to create two distinct temperature zones in the furnace and thermally dissociate the  $\text{Bi}_2$  in the hotter central zone,  $T_2$  shown in Fig. 6. It is not possible just by increasing the temperature to lower the percentage of dimers in the vapor. Although an increase in temperature will increase the dissociation of the molecule, an increase in temperature also causes an increase in total pressure, which forces the reaction  $\text{Bi}_2 \rightleftharpoons 2 \text{Bi}$  to the left. Alternatively, in the language of thermodynamics, the  $T\Delta S$  term dominates over the  $\Delta H$  term. Heat pipes, however, allow us to set the total bismuth pressure in the system at  $\sim 1$  torr ( $900^\circ\text{C}$ ) and raise just the central portion of the laser tube to  $1500^\circ\text{C}$ . This is sufficient to thermally dissociate  $\text{Bi}_2$  so that the fraction of dimers in the central region is less than 0.4% which is the dimer concentration in copper vapor at 1 torr equilibrium pressure. The

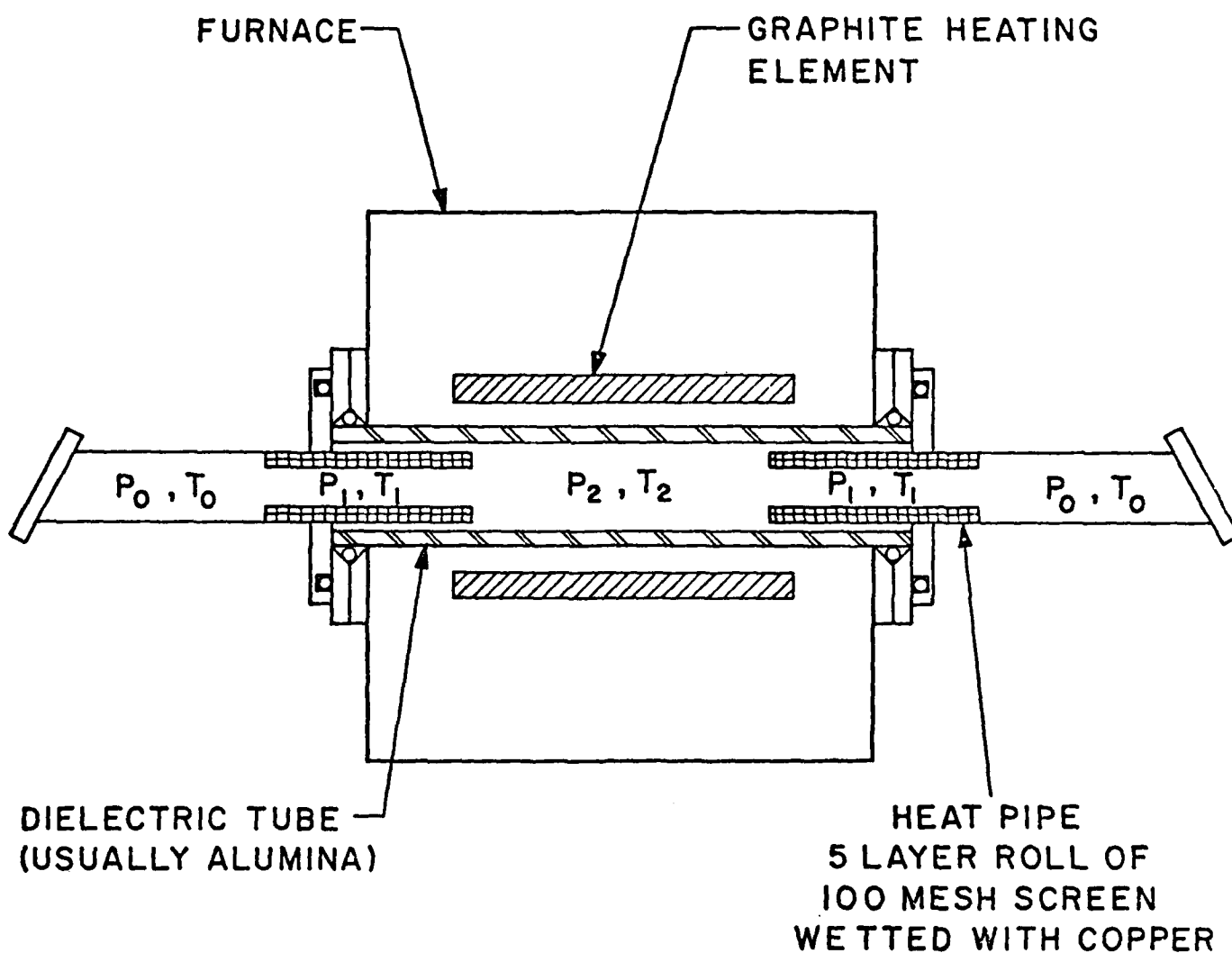


Fig. 6 Split heat-pipe apparatus to establish two distinct temperature zones in the furnace.

decrease in dimer concentration of bismuth vapor in the hotter central zone as its temperature is raised is indicated in Table 4. The temperature of the split heat-pipe is held at  $900^{\circ}\text{C}$  so that the pressure throughout remains constant;  $P_0=P_1=P_2=1$  torr. The values calculated in Table 4 are based on Hultgren's <sup>20</sup> values both of dimer concentration plotted in Fig. 3 and of total bismuth vapor pressure plotted in Fig. 4 as the thermal equilibrium values at each temperature.

TABLE 4

Thermal Dissociation of Bismuth Dimers in the Split Heat-Pipe Apparatus of Figure 6. The end zones are held at  $900^{\circ}\text{C}$  corresponding to a total, equilibrium, bismuth vapor pressure of 1 torr and the temperature of the central zone is increased.

$T_1$	$T_2$	DIMER CONCENTRATION
$900^{\circ}\text{C}$	$900^{\circ}\text{C}$	53%
$900^{\circ}\text{C}$	$1100^{\circ}\text{C}$	11%
$900^{\circ}\text{C}$	$1300^{\circ}\text{C}$	1.4%
$900^{\circ}\text{C}$	$1500^{\circ}\text{C}$	0.3%

When thermal dissociation was experimentally tested, establishment of two distinct temperature zones was evident. The temperature along the 6" long tungsten-mesh split heat-pipe was examined by means of an optical pyrometer. The temperature indicated along the inside of the mesh tube was uniform confirming the wicking action of liquid bismuth. The split heat-pipe also served as electrodes for the electric discharge. No evidence of laser action at  $4722\text{\AA}$  was observed, however.

## 7. DISCHARGE DISSOCIATION OF BISMUTH DIMERS

A double-pulse discharge system was also tried - the first pulse to dissociate the molecules and the second to excite the Bi atoms. This method was first demonstrated by Chen, Nerheim and Russell<sup>36</sup> to obtain laser action in atomic copper using copper chloride vapor.

The hot-window discharge system utilized for these double-pulse experiments is shown in Fig. 7. Electrodes, a valve and quartz window-to-tube seals all capable of withstanding temperatures as high as 1000°C were developed to construct a system in which the entire laser tube can be operated at temperatures up to the 1000°C devitrification limit of quartz. The entire laser discharge tube can operate then, under equilibrium temperature and vapor density conditions; and the operational lifetime is no longer limited by migration of the active material out of the hot zone.

The quartz laser discharge tube (2mm i. d., 20cm long with quartz Brewster-angle windows fused to the tube) was connected to a sidearm, as indicated in Fig. 7, which contained 0.2 gms of copper chloride (Alpha Products, stock #87376, lot #102373) and 1.25 gms of bismuth shot (United Minerals and Chemicals, 99.999% pure). The sidearm was placed in a second furnace to independently control its temperature and thereby the vapor pressure of its contents. The optical cavity consisted of an aluminized concave mirror (172.4cm radius) and a flat beamsplitter (63% transmission) separated by 120cm.

The double-pulse discharge system is shown in Fig. 8. Two Sprague 3900 pF ceramic capacitors charged to 12kV were independently discharged through the laser tube by separate 5948 hydrogen thyratrons. The pulse generators provide an adjustable delay time between the two pulses as well as an adjustable repetition rate of the double-pulse signal.

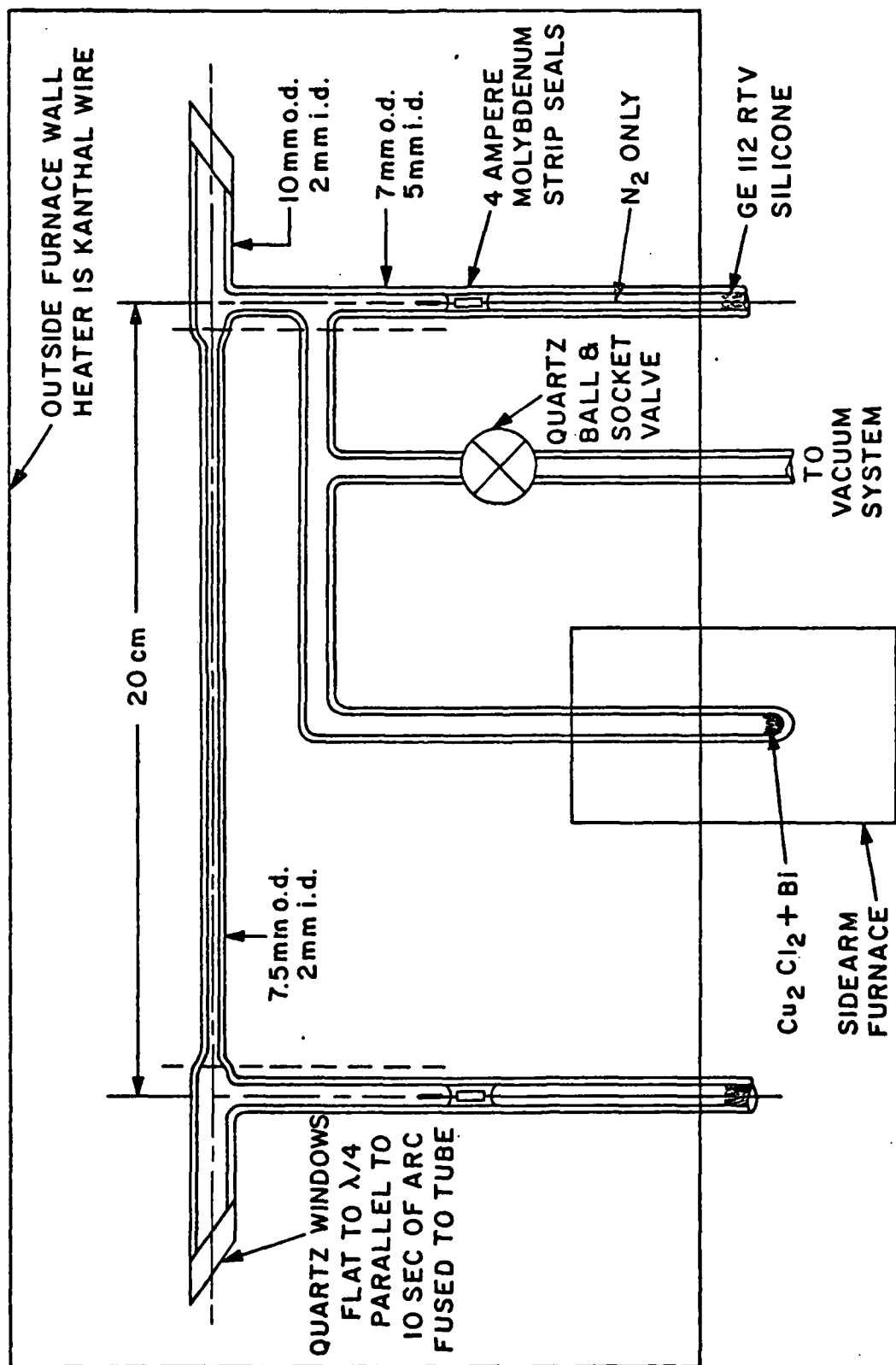


Fig. 7 Hot-window quartz-tube laser-discharge apparatus capable of sustained operation at temperatures up to 1000°C for copper halide and bismuth dimer vapors.



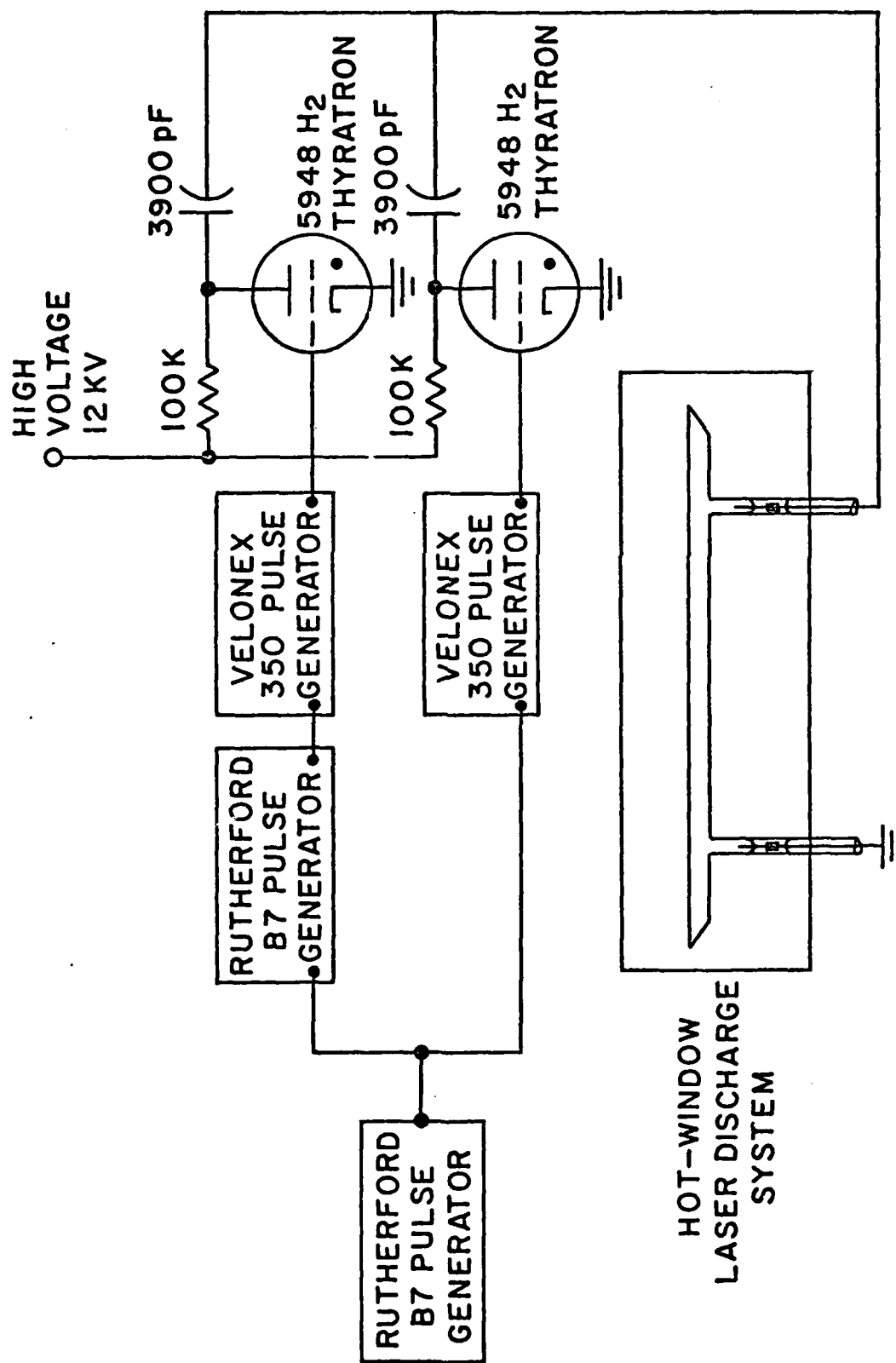


Fig. 8 Double-pulse excitation system for copper halide and bismuth dimer vapors.

The small amount of copper chloride was included in the sidearm along with bismuth to demonstrate the efficacy of double-pulse excitation in our experimental system. When the temperature of the main and sidearm furnaces was raised to  $500^{\circ}\text{C}$ , laser action was observed on the  $5105\text{\AA}$  and  $5782\text{\AA}$  atomic copper transitions. Optimum delay time between pulses was 28-30  $\mu\text{sec}$ . The pressure range in which the laser would operate was 3-5 torr of argon with the optimum being 3.8 torr. Peak current amplitudes were 13 and 15 amperes respectively for the two pulses, corresponding to peak current densities of 400 to  $500\text{ A/cm}^2$ . The copper vapor laser action was also used to optimize the optical cavity alignment.

When the temperature of the furnaces were raised above  $700^{\circ}\text{C}$ , the copper chloride diffused through the open quartz ball and socket valve and bismuth took over the discharge. The furnace temperatures were gradually taken as high as  $970^{\circ}\text{C}$  corresponding to an equilibrium total bismuth vapor pressure of 2.7 torr. Helium and argon were used as buffer gases and tested throughout a pressure range of 0-500 torr. The peak current amplitudes were operated up to 20 amperes ( $600\text{ A/cm}^2$ ). The time delay between pulses was usually set at 30  $\mu\text{sec}$ . When the delay was varied, the output light signal at  $4722\text{\AA}$  produced by the second pulse never increased from its value at 30  $\mu\text{sec}$ . The output light pulses were examined by means of a Jarrell-Ash 0.5m spectrometer which was usually set at  $4722\text{\AA}$ . An iris in front of the spectrometer was adjusted to narrow the field of view to that of the back mirror of the laser resonator as viewed through the 2mm i. d. discharge tube.

No evidence of laser action at  $4722\text{\AA}$  was observed during any variation of experimental parameters. The amplitude of the output light signal at  $4722\text{\AA}$  produced by the second discharge pulse was usually equal to or less than that produced by the first pulse. It was never more than 20% larger than the first. Even more disheartening was the observation that the output light pulses did not change when the back mirror was blocked. This indicates that the discharge was not transparent at  $4722\text{\AA}$ .

Both the thermal dissociation and discharge dissociation methods were successful, we believe, in substantially reducing the proportion of dimers in the vapor of bismuth. The absence of enhancement of light output signal at  $4722\text{\AA}$  and the lack of transparency of the discharge at the proposed laser transition in spite of an estimated reduction in dimer mole fraction in the vapor by 100 suggests that other processes are more important in populating the  $^2D_{3/2}$  metastable, proposed, lower laser level. We conclude, therefore, that the presence of dimers in the vapor of bismuth is not the dominant explanation for the absence of laser action at  $4722\text{\AA}$ .

## 8. COMPETING PROCESSES

The bismuth atom has three 6p valence electrons. All previously-demonstrated pulsed atomic-vapor lasers have only one or two valence electrons. Therefore in bismuth, there are more competing channels both for excitation from the ground level and radiative filling of the proposed, metastable, lower laser level. This is illustrated in Fig. 9 where in the upper third of the figure the proposed laser at  $4722\text{\AA}$  in bismuth, displayed on a bismuth energy level diagram, is compared with the pulsed copper atomic laser transitions at  $5105\text{\AA}$  and  $5782\text{\AA}$  displayed on a copper energy level diagram.

In the middle third of Fig. 9, the Corliss-Bozman<sup>10</sup> measured oscillator strengths for transitions out of the ground levels are indicated on arrows to the respective levels in bismuth and copper. The  $f$  values can be used as an indication of the electron excitation cross section of the various excited levels. Notice that in copper the sum of the  $f$  values to the two upper laser levels divided by the sum of all measured  $f$  values out of the ground level is  $(.320 + .155)/.529 = 90\%$  while in bismuth it is only 56%. Furthermore there are several 6p  $\rightarrow$  6d transitions in bismuth for which  $f$  values are not found in Corliss-Bozman, and when included may reduce the 56% ratio. In copper, however, all unmeasured lines terminate on highly excited levels and therefore have very small  $f$  values which would not significantly affect the 90% ratio.

In the lower third of Fig. 9 Corliss-Bozman spontaneous-emission transition probabilities are indicated on arrows for all measured lines terminating on the metastable, proposed lower laser levels. In copper there are fewer lines and their  $A$  values are generally small. In bismuth, however, there

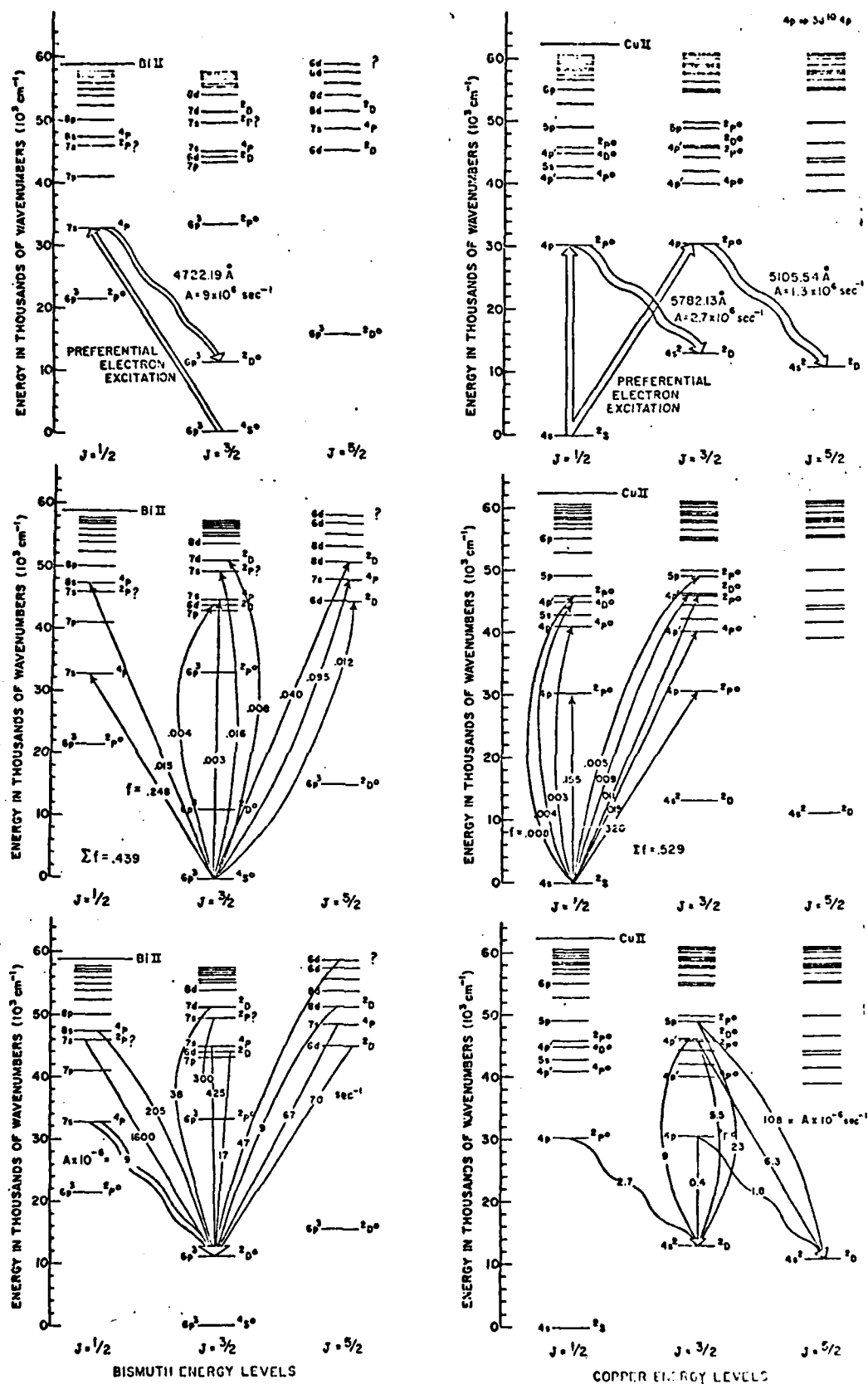


Fig. 9 Comparison of the situation in bismuth with that in copper for a) expected pulsed laser action, b) oscillator strengths ( $f$  values) out of the ground levels and c) radiative filling ( $A$  values) of the proposed, metastable, lower laser levels.

are many lines most of which have A values substantially larger than that of the proposed  $4722\text{\AA}$  laser line. Several of these lines arise from excited levels which have moderately strong f value connections with the ground level. Fluorescence studies we carried out confirmed this situation. We observed at least nine transitions in addition to the proposed laser transition at  $4722\text{\AA}$  which also terminate on the  $^2D_{3/2}$  proposed, lower laser level. Although none was as intense as the  $4722\text{\AA}$  spontaneous emission, in sum these other nine lines appeared to contribute to the population of the  $^2D_{3/2}$  level to the same or larger extent as the  $4722\text{\AA}$  line did. Because of the larger transition probabilities of almost all of these lines, they could have prevented the establishment of a population inversion on the  $4722\text{\AA}$  transition.

#### 9. COMPUTER MODELING

A computer modeling approach is required for an analysis of the effect of competing processes on potential laser action at  $4722\text{\AA}$  because of the large number of excitation and relaxation channels as well as the large number of bismuth atomic energy levels involved. A computer model of the dynamics of pulsed, atomic vapor lasers has been developed and is described in Appendix II. The model includes rate equations for the population of as many as 15 energy levels of the laser species which may be directly or indirectly involved in the development of laser action. Also included are rate equations for the population of an additional species which is modeled by two energy levels - ground state atomic and ionic levels. This species, usually argon, is present to act as a buffer gas and to facilitate electrical breakdown and discharge.

Primary excitation in the model is provided by electron collisions. Relaxation processes are electron de-exciting collisions, radiative relaxation and

diffusion to and de-excitation at the walls of the container. The rate constants for transitions between the various energy levels and for ionization depend on the cross sections for these processes and on the electron number density and energy distribution. The electron energy distribution is assumed to have a Maxwell-Boltzmann distribution throughout the discharge pulse, but the average energy is permitted to change as determined by an energy balance equation. Since in most cases the cross sections for ionization or for excitation are not known, they have been estimated using the semiclassical formulas of Gryzinski.

The computer model was applied to the situation in bismuth using the lowest 15 atomic energy levels and the ground level of  $\text{Bi}^+$  from Moore's tabulation<sup>37</sup> and the transition probabilities of Corliss and Bozman.<sup>10</sup> Radiation trapping was included. Where values of radiation transition probabilities had not been measured, a wall collision relaxation rate of  $10^3 \text{ sec}^{-1}$  was assumed. Fig. 10 shows a computer print-out for the time development of the absolute magnitude of the capacitor voltage (V), the discharge tube current density (I) and the blue laser output anticipated at  $4722\text{\AA}^0$  (\*). The computer print-out models the situation where a 2000pF capacitor charged to 15kV has suddenly been applied to a discharge tube 2.5 cm diameter with a hot zone 25 cm long containing  $10^{15}$  Bi atoms/cm<sup>3</sup> and  $2 \times 10^{16}$  argon atoms/cm<sup>3</sup>. A circuit inductance of 1 $\mu$ H has been assumed as well as a laser cavity time constant of 3.3 nsec. To facilitate identification of the expected laser output at  $4722\text{\AA}^0$ , a solid line has been drawn through the computer-generated points (\*). The vertical full scale values are 15kV voltage, 100 amperes/cm<sup>2</sup> current density and 50 kW laser output power. The full scale horizontal value is 100 nano-seconds.

1.5000E+04  
1.4238E-03  
1.5435E-11

1.9695E+01  
2.9543E+00  
7.4745E-09  
2.2525E-09  
1.1024E-09  
6.9214E-10

1.9695E+01  
2.9543E+00  
7.4745E-09  
2.2525E-09  
1.1024E-09  
6.9214E-10

1.9695E+01  
2.9543E+00  
7.4745E-09  
2.2525E-09  
1.1024E-09  
6.9214E-10

1.9695E+01  
2.9543E+00  
7.4745E-09  
2.2525E-09  
1.1024E-09  
6.9214E-10

1.9695E+01  
2.9543E+00  
7.4745E-09  
2.2525E-09  
1.1024E-09  
6.9214E-10

1.9695E+01  
2.9543E+00  
7.4745E-09  
2.2525E-09  
1.1024E-09  
6.9214E-10

1.9695E+01  
2.9543E+00  
7.4745E-09  
2.2525E-09  
1.1024E-09  
6.9214E-10

1.9695E+01  
2.9543E+00  
7.4745E-09  
2.2525E-09  
1.1024E-09  
6.9214E-10

VSCALE = 1.500E+04 VOLTS  
ISCALE = 1.000E+02 AMP/CM2

PSCALE = 5.000E+04 WATTS

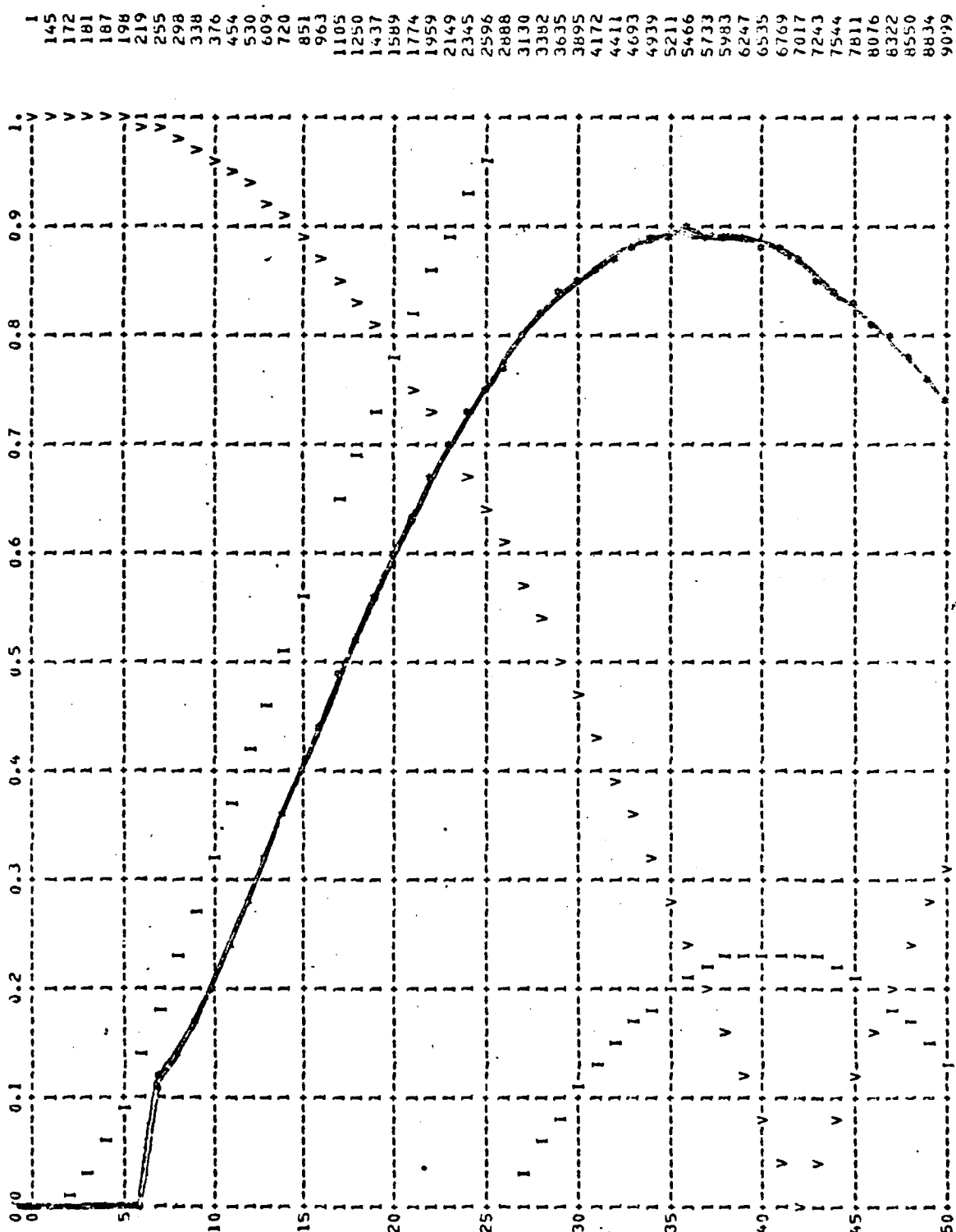


Fig. 10 Computer modeling of a pulsed discharge in bismuth vapor where the capacitor voltage (V), discharge tube current density (I) and expected 4722Å laser output (\*) are shown as a function of time. Gryzinski cross sections are used.



It is evident in Fig. 10 that in spite of the competing processes within the bismuth atom, the computer model predicts that a population inversion will be obtained in the  $4722\text{\AA}$  transition under conditions which simulate our experimental apparatus. The peak intensity of the expected laser pulse is 45kW and full width at half maximum intensity  $\sim 90$  nsec.

#### 10. ELECTRON EXCITATION CROSS SECTIONS OF THE PROPOSED BISMUTH LASER LEVELS

An experimental determination of electron impact cross sections both for excitation of the upper  $^4P_{1/2}$  and of the lower  $^2D_{3/2}$  levels of bismuth has been made by Williams, Trajmar and Bozinis<sup>38</sup> (WTB) and became available in May 1975. Unfortunately the WTB measurements were carried out only at an electron energy of 40eV, whereas production of a population inversion in a pulsed discharge will be determined by the cross section values at much lower electron energies. Nevertheless a comparison of the Gryzinski calculation with the WTB measurement may still be illustrative. At 40eV our Gryzinski calculation of the electron excitation cross sections of the proposed upper laser level ( $^4P_{1/2}$ ) was approximately one-half that of the WTB value and our Gryzinski estimate of the cross section for electron excitation of the lower laser level ( $^2D_{3/2}$ ) was approximately  $1/30$  that of the WTB value. We then treated our Gryzinski results as relative excitation curves and used the WTB values to normalize them at 40eV; that is, we increased our upper laser level excitation rates by a factor of 2 and our lower level excitation rates by a factor of 30 throughout the entire electron energy range.

Fig. 11 indicates that a strong laser output would still be expected under these conditions. Although the expected peak laser output decreased from 45 to 30kW as a result of the change in electron excitation cross sections, it is still stronger than the modeling results for the copper laser output under the

BEST AVAILABLE COPY

1.08099E+03  
9.43160E-11

7.30626E+06  
6.92146E-10

7.08582E+08  
1.10242E-09

1.96950E+01  
2.25250E-09

2.95436E+00  
7.47457E-09

1.96950E+01  
3.58139E-08

1.30615E-03  
2.33917E-12

1.54352E-11  
1.16495E-11

TS SCALE = 2.000E-09 SEC.

VSCALE = 1.500E+04 VOLTS ISCALE = 1.000E+02 AMP/CM2

PSCALE = 5.000E+04 WATTS

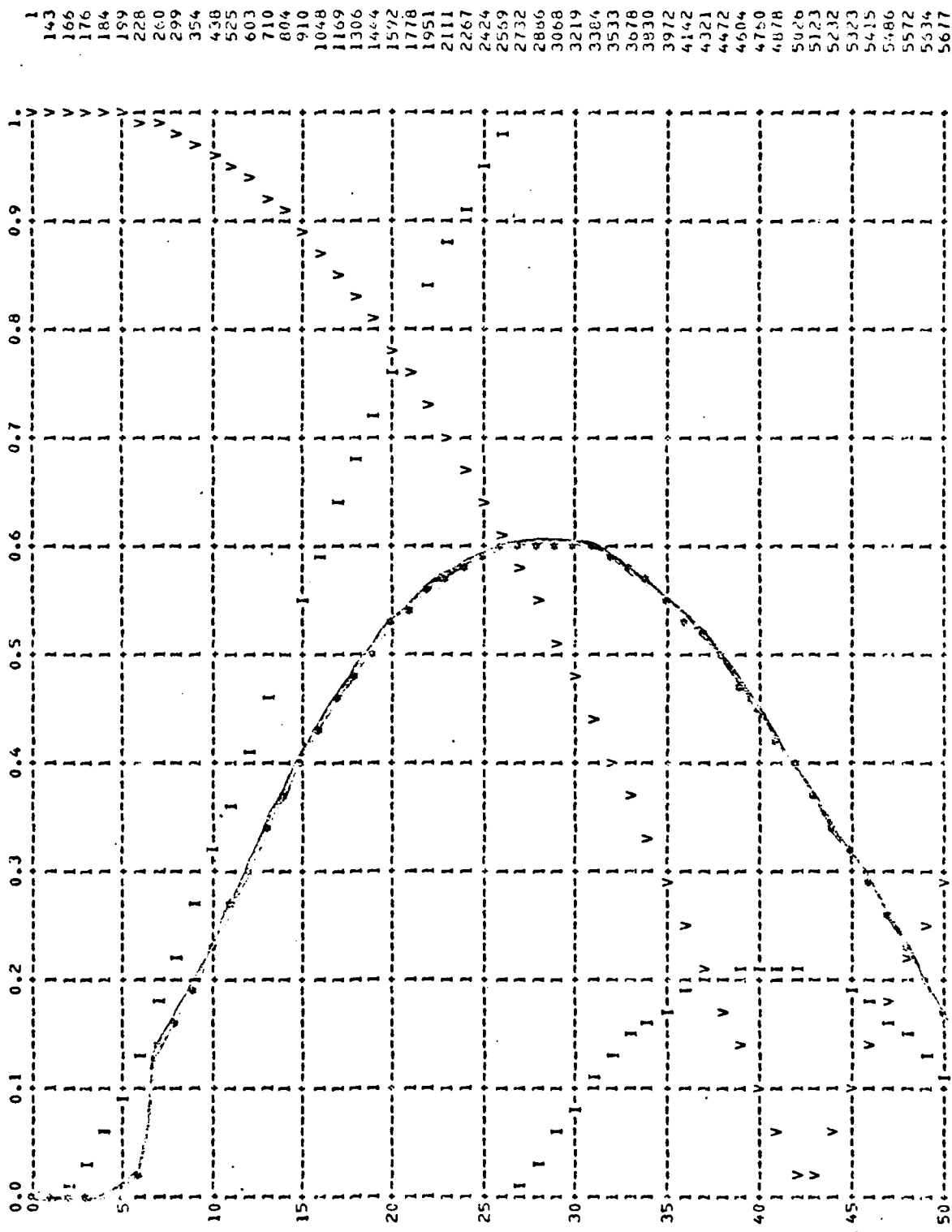


Fig. 11 Computer modeling of a pulsed discharge in bismuth vapor where the capacitor voltage (V), discharge tube current density (I) and expected 4722 Å laser output (\*) are shown as a function of time. Gryzinski cross sections have been normalized to WTB values at 40 eV.

same conditions. There is no justification, therefore, for the statement "... only a small population inversion can be obtained with 40eV electrons" which was made by WTB in Reference 38. The ratio of the WTB values for upper and lower excitation cross sections, which is 13:1, is entirely consistent with production of a substantial population inversion. In fact we shall now show that it is quite likely that the WTB results for bismuth are quite similar to their values for copper<sup>39</sup> and lead,<sup>40</sup> and both of these vapors have furnished strong pulsed laser action.

First it should be noted that the estimate made by WTB of bismuth molecules in the vapor (14%) is too low by a factor of 4 as shown in Section 4 of this report. More important, however, WTB normalized their electron excitation cross sections to Lvov's value<sup>12</sup> for the  $3067\text{\AA}$  resonance transition oscillator strength. In Section 3 of this report it was shown that Lvov's  $f$  value is too low by a factor of 2. Therefore the WTB values<sup>38</sup> as reported for electron excitation of both the upper  $^4P_{1/2}$  and of the lower  $^2D_{3/2}$  levels of bismuth should be increased by a factor of 2. On the other hand the Williams-Trajmar (WT) reported values<sup>39</sup> for electron excitation of the upper  $^2P_{3/2}$  and lower  $^2D_{5/2}$  levels in copper have been reported<sup>41</sup> to be too large by at least a factor of 7. After these changes are made, the corrected values for integral electron excitation cross sections of the upper and lower laser levels in copper, lead and bismuth are compared in Table 5.

TABLE 5

Comparison of integral electron excitation cross sections (in units of  $10^{-16} \text{ cm}^2$ ) for the upper and lower laser levels in atomic copper, lead and bismuth using corrected WTB<sup>38</sup> and WT<sup>39,40</sup> values as described in the text.

	Incident Electron Energy		
	20eV	40eV	60eV
	( $10^{-16} \text{ cm}^2$ )	( $10^{-16} \text{ cm}^2$ )	( $10^{-16} \text{ cm}^2$ )
Upper Laser Levels			
Cu( $^2\text{P}_{3/2, 1/2}$ )	11.0		5.2
Pb( $^3\text{P}_1$ )		8.4	
Bi( $^4\text{P}_{1/2}$ )		7.6	
Lower Laser Levels			
Cu( $^2\text{D}_{5/2}$ )	0.26		0.051
Pb( $^1\text{D}_2$ )		0.050	
Bi( $^2\text{D}_{3/2}$ )		0.58	

Table 5 indicates that the electron excitation cross section of the resonance levels of the three metals Cu, Pb and Bi are quite comparable at 40eV. Excitation cross sections of the metastable lower laser levels are considerably smaller for all three metals at 40eV. Although the metastable level excitation cross section is larger for Bi than for Cu or Pb, it is still so much smaller than the resonance level excitation cross section that if the pulsed discharge consisted entirely of 40eV electrons 93% of the Bi atoms excited to one of these two levels would be in the upper laser level.

We have already pointed out that it is the electron excitation cross sections at lower electron energies (1-10eV) which will determine the direct production of a population inversion at  $4722\text{\AA}^0$  in a pulsed discharge in bismuth. The present state of knowledge of electron excitation cross sections of the upper  $^4P_{1/2}$  and lower  $^2D_{3/2}$  levels is entirely consistent with the generation of strong laser action at  $4722\text{\AA}^0$  and provides no basis to account for its absence.

#### 11. ELECTRON COLLISIONAL MIXING BETWEEN LASER LEVELS

In Leonard's computer modeling<sup>42</sup> of the copper vapor laser, the electron collisional mixing rate between laser levels appeared to be the limiting process. These electron collisions-of-the-second-kind deactivate copper atoms already in the upper laser level to the lower laser level. We are presently assessing the importance of this process in copper.

In bismuth, an electron collisional mixing rate was not included in either Fig. 10 or Fig. 11. An electron collisional mixing rate was then included in the computer run whose print-out is shown in Fig. 12. Fig. 12 is identical, for all practical purposes, to that of Fig. 11. To the extent that we have modeled the electron collisional mixing between laser levels correctly, they do not explain the absence of laser action at  $4722\text{\AA}^0$  in bismuth.

#### 12. A POSSIBLE EXPLANATION FOR ABSENCE OF LASER ACTION

We have already shown it is unlikely that the absence of laser action at  $4722\text{\AA}^0$  in bismuth vapor can be accounted for by any of the first three explanations considered;

- (1) too slow a risetime of the excitation current pulse, or
- (2) the presence of bismuth dimers in the vapor or
- (3) an unfavorable ratio of the electron excitation cross sections for the  $^4P_{1/2}$  resonance and  $^2D_{3/2}$  metastable levels.

1.50000E+04  
1.42398E-03  
1.54352E-11

1.96958E+01  
2.95436E+00  
7.47878E-09  
2.25250E-09  
3.44780E-33  
2.000E-09 SEC.

1.96958E+01  
2.95436E+00  
7.47878E-09  
2.25250E-09  
3.44780E-33  
2.000E-09 SEC.

1.96958E+01  
2.95436E+00  
7.47878E-09  
2.25250E-09  
3.44780E-33  
2.000E-09 SEC.

1.96958E+01  
2.95436E+00  
7.47878E-09  
2.25250E-09  
3.44780E-33  
2.000E-09 SEC.

1.96958E+01  
2.95436E+00  
7.47878E-09  
2.25250E-09  
3.44780E-33  
2.000E-09 SEC.

1.96958E+01  
2.95436E+00  
7.47878E-09  
2.25250E-09  
3.44780E-33  
2.000E-09 SEC.

1.96958E+01  
2.95436E+00  
7.47878E-09  
2.25250E-09  
3.44780E-33  
2.000E-09 SEC.

1.96958E+01  
2.95436E+00  
7.47878E-09  
2.25250E-09  
3.44780E-33  
2.000E-09 SEC.

VSCALE = 1.500E+04 VOLTS  
ISCALE = 1.000E+02 AMP/CM2

PSCALE = 5.000E+04 WATTS

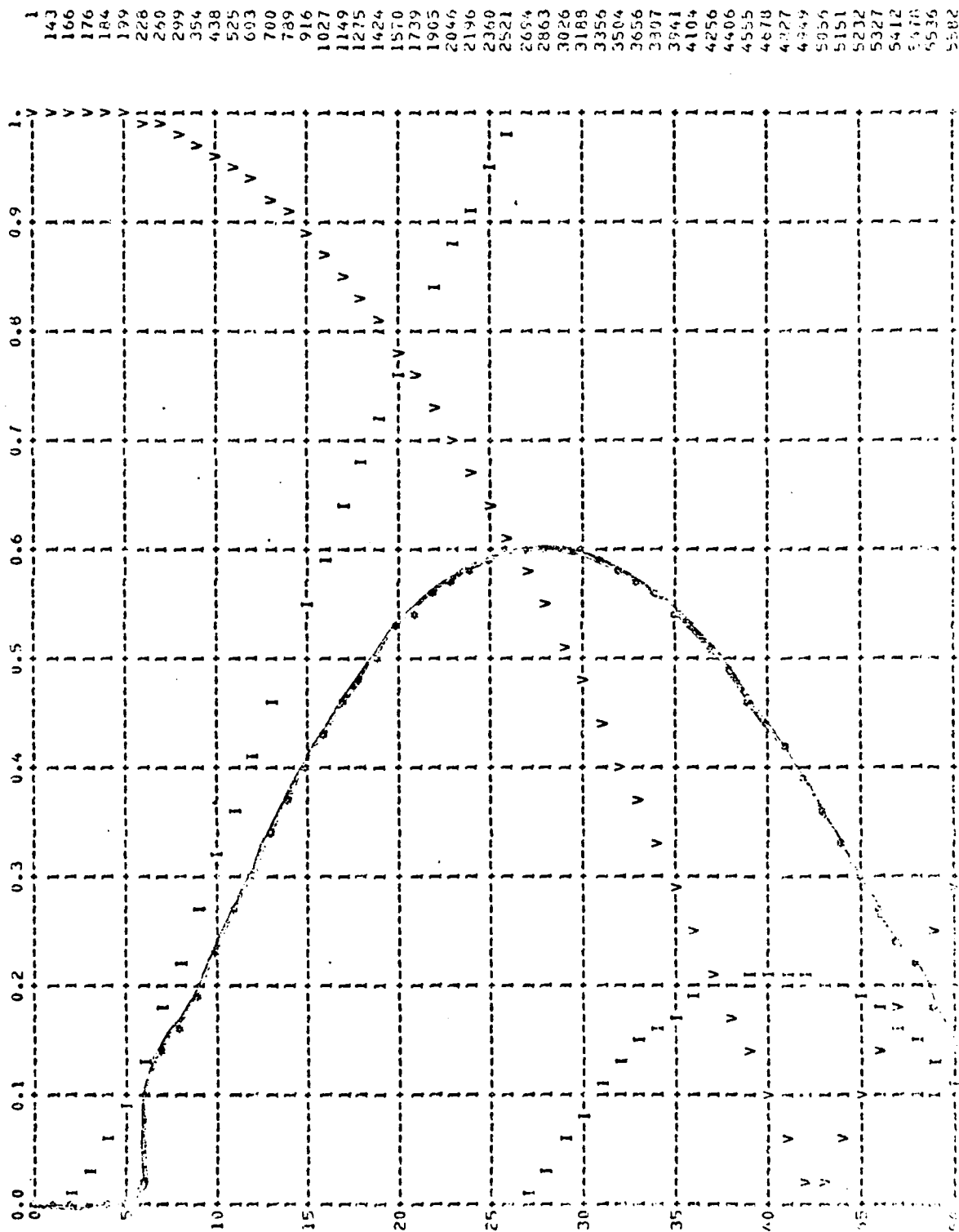


Fig. 12 Electron collisional mixing between laser levels has been added to the computer modeling shown in Fig. 11.

Thus far explanation (4), competing processes within the Bi atom also has not provided an answer. The computer modeling results displayed in Fig. 10 indicate that utilization of Corliss-Bozman transition probabilities to model the rates of competing processes does not substantially reduce the population inversion expected. The possibility of significant errors in the Corliss-Bozman transition probabilities has already been mentioned in Section 3. The Corliss-Bozman values for the strong competing channels should therefore be carefully examined.

The direct laser excitation channel is electron excitation of the  $^4S_{3/2} \rightarrow ^4P_{1/2}$  transition. On the basis of LS coupling, the strengths of competing excitation channels  $^4S_{3/2} \rightarrow ^4P_{3/2}$  and  $5/2$  would be expected to be  $2/3$  and  $1/3$  respectively of that of the direct laser excitation channel. The Corliss-Bozman  $gA$  values can be converted to Condon-Shortley line strengths <sup>43</sup> by

$$S(J, J') = 4.936 \times 10^5 \lambda^3 gA.$$

The relative Corliss-Bozman line strengths for the  $6p^3 \ ^4S_{3/2} \rightarrow 6p^2 7s \ ^4P_{1/2, 3/2, 5/2}$  multiplet then are; 1: .008: .26. Compared with the LS coupling line strength of 1: .667: .333, we see that the strength of the  $^4S_{3/2} \rightarrow ^4P_{3/2}$  transition is 80 times weaker than expected.

When the Corliss-Bozman values for the similar transitions are examined in antimony and arsenic, the elements above bismuth in column VA of the periodic table, the  $^4S_{3/2} \rightarrow ^4P_{3/2}$  member of the multiplet is not observed to be substantially weaker than the other two components. For Sb the Corliss-Bozman relative line strengths for the  $5p^3 \ ^4S_{3/2} \rightarrow 5p^2 6s \ ^4P_{1/2, 3/2, 5/2}$  multiplet are; 1: 1.39: 3. For As the Corliss-Bozman relative line strengths for the  $4p^3 \ ^4S_{3/2} \rightarrow 4p^2 5s \ ^4P_{1/2, 3/2, 5/2}$  multiplet are; 1: .67 (not measured).

The intermediate coupling calculations of transition probabilities for these multiplets<sup>17, 18</sup> can also be used to calculate line strengths. Intermediate coupling line strengths are listed in Table 6 for comparison with the Corliss-Bozman line strengths and the LS coupling relative line strengths.

TABLE 6

Comparison of Line Strengths for the resonance multiplets of arsenic, antimony and bismuth.  $S_{CB}$  are calculated from Corliss-Bozman's values in Reg. 10.  $S_{DV}$  and  $S_{DL}$  are calculated from Holmgren's values in Ref. 17 for dipole velocity and dipole length approximations.  $S_{KM}$  are calculated from Kunisz and Mizdalek's values in Ref. 18.

	$^4S_{3/2} \rightarrow ^4P_{1/2}$	$^4S_{3/2} \rightarrow ^4P_{3/2}$	$^4S_{3/2} \rightarrow ^4P_{5/2}$
LS Coupling Relative S	1.000	0.667	0.333
As( $4p^3 \rightarrow 4p^2 5s$ )			
$\lambda$	1972 Å	1937 Å	1890 Å
$S_{CB}$	1.89	1.26	-
$S_{DV}$	.848	1.64	2.30
$S_{DL}$	1.51	2.84	4.00
Sb( $5p^3 \rightarrow 5p^2 6s$ )			
$\lambda$	2312 Å	2176 Å	2069 Å
$S_{CB}$	.915	1.27	2.75
$S_{DV}$	1.20	1.95	2.50
$S_{DL}$	2.45	3.93	4.93
Bi( $6p^3 \rightarrow 6p^2 7s$ )			
$\lambda$	3067 Å	2228 Å	2062 Å
$S_{CB}$	9.97	0.076	2.60
$S_{DV}$	3.82	1.55	2.27
$S_{DL}$	6.75	2.64	3.61
$S_{KM}$	4.82	4.79	.343



Table 6 reveals that the Corliss-Bozman line strength for the  $2228\text{\AA}$   $^4S_{3/2} \rightarrow ^4P_{3/2}$  transition in Bi is surprisingly small on the basis of the following comparisons. First, Holmgren's intermediate coupling line strengths for the  $^4S_{3/2} \rightarrow ^4P_{3/2}$  transitions in As, Sb and Bi are comparable (within a factor of 2.5) with the  $^4S_{3/2} \rightarrow ^4P_{1/2}$  line strengths regardless of whether dipole velocity or dipole length approximations are used.

Second, the intermediate coupling line strengths of Kunisz and Mizdalek for the  $^4S_{3/2} \rightarrow ^4P_{1/2}$  and  $^4S_{3/2} \rightarrow ^4P_{3/2}$  transitions in Bi are nearly identical. Furthermore, Corliss and Bozman's line strengths for 7 of the 8 transitions observed in As, Sb and Bi (i. e., all except for the  $2228\text{\AA}$  Bi transition) are within a factor of 3 of the intermediate coupling line strengths of Holmgren using either the dipole velocity or dipole length approximations. The Corliss-Bozman line strength of the  $2228\text{\AA}$   $^4S_{3/2} \rightarrow ^4P_{3/2}$  in Bi, however, is at least 20 times smaller than the intermediate coupling line strengths. All indications are, therefore, that this Corliss-Bozman value is anomalously small.

The spectroscopic evidence, both in terms of calculations for Bi as well as calculations and measurements for the analogous elements As and Sb, indicates that the  $6p^3\ ^4S_{3/2} \rightarrow 6p^27s\ ^4P_{3/2}$  transition in Bi is a strong transition. Significant electron excitation of the  $6p^27s\ ^4P_{3/2}$  level may be expected, therefore, during a pulsed discharge in bismuth vapor. This expectation is supported by the energy loss spectrum for 40eV electrons incident upon a bismuth vapor beam, which has been measured by Williams, Trajmar and Bozinis<sup>38</sup> (WTB) and is displayed in Fig. 13.

The first large peak in Fig. 13 must correspond to excitation of the  $6p^27s\ ^4P_{1/2}$  resonance level at 4.04eV and direct excitation of the proposed upper laser level. The other possibility, the  $6p^3\ ^2P_{3/2}$  level at 4.11eV, is

40

The WTB energy loss spectrum in Fig. 13 confirms the spectroscopic- based conclusions of preceding paragraphs based on Table 6. During a pulsed discharge, therefore, the  $6p^2 7s \ ^4P_{3/2}$  level may be expected to be populated at a rate comparable to that of the  $^4P_{1/2}$  level. As indicated in Figs. 2 and 9 and Table 7 spontaneous radiation at  $2989\text{\AA}$  is expected to be very strong, stronger than the  $4722\text{\AA}$  spontaneous radiation, and therefore can seriously interfere with the establishment of the proposed population inversion. Although the several  $gA$  values given in Table 7 for the  $2989\text{\AA}$  and  $2697\text{\AA}$  lines are not as consistent as they are for the  $4722\text{\AA}$  line (variations of 57 and 40 compared with 2) they still suggest that spontaneous radiation of these first two lines will be much more effective in populating the  $^2D_{3/2}$  proposed lower laser level than will spontaneous radiation at  $4722\text{\AA}$ .

TABLE 7

Comparison of Spontaneous Radiation rates into the  $^2D_{3/2}$  proposed lower laser level from the  $^4P_{1/2, 3/2, 5/2}$  resonance levels.  $gA_{CB}$  are Corliss-Bozman's values from Ref. 10.  $gA_{DV}$  and  $gA_{DL}$  are Holmgren's values from Ref. 17 for dipole velocity and dipole length approximations.  $gA_{KM}$  are Kunisz and Migdalek's values from Ref. 18. (The tabulated values are in units of  $10^8$  photons/sec.)

	$^4P_{1/2} \rightarrow ^2D_{3/2}$ $4722\text{\AA}$ ( $10^8/\text{sec}$ )	$^4P_{3/2} \rightarrow ^2D_{3/2}$ $2989\text{\AA}$ ( $10^8/\text{sec}$ )	$^4P_{5/2} \rightarrow ^2D_{3/2}$ $2697\text{\AA}$ ( $10^8/\text{sec}$ )
$gA_{CB}$	.18	17.	4.0
$gA_{DV}$	.132	1.16	.10
$gA_{DL}$	.099	2.72	.41
$gA_{KM}$	.091	.30	1.57

The most likely explanation for the absence of laser action at  $4722\text{\AA}$  in bismuth vapor appears to be that the Corliss-Bozman transition probability for the  $2228\text{\AA}$   $4\text{P}_{3/2} - 4\text{S}_{3/2}$  Bi line is too low by at least a factor of 20. Strong population of the  $6\text{p}^2 7\text{s}$   $4\text{P}_{3/2}$  resonance level during a pulsed discharge and strong spontaneous radiation at  $2989\text{\AA}$  then fills the  $6\text{p}^3 2\text{D}_{3/2}$  metastable level and prevents the build-up of a sufficient population inversion on the  $4722\text{\AA}$  line. The computer modeling studies should be continued to verify this hypothesis. Such computer modeling will also be helpful in evaluating the possibilities of similar potentially-efficient laser transitions in other atomic vapors.

### 13. MODELING OF THE INITIAL BREAKDOWN PROCESS

During the initial nanosecond after the fast thyatron switch closes suddenly applying a charged capacitor across the discharge tube, the resistivity of the discharge tube drops sharply as the electron density builds up from a very low level, determined by the Saha equation ( $\sim 20\text{ cm}^{-3}$ ) or left over from the previous pulse ( $> 10^2\text{ cm}^{-3}$ ), to a level characteristic of a very weak discharge ( $10^9 - 10^{10}\text{ cm}^{-3}$  or greater). Because the energy dissipated in the discharge ( $j^2 R$ ) is shared by so few electrons, the electron temperature reaches unphysically high values during the computer modeling of this initial breakdown process.

Additional computer modeling should be carried out to assess the effect of the breakdown process during the initial nanosecond on subsequent laser action. The very limited amount of work which could be carried out during this study indicated that this may be a most important mechanism, whose optimization could produce substantial changes in the laser output of the general class of pulsed atomic vapor lasers.

#### 14. SUMMARY AND CONCLUSIONS

At the outset of this investigation, the presence of dimers in bismuth vapor appeared to be the likely explanation for the absence of laser action at  $4722\text{\AA}$ . Discordant values for bismuth vapor pressure and composition were critically evaluated as indicated in Figs. 3 and 4. Both thermal dissociation and discharge dissociation of the dimers were experimentally investigated, and each method failed to produce laser action.

Our investigation was then expanded to examine other possible explanations. We constructed a radial discharge apparatus and reduced the risetime of the excitation current pulse to  $\sim 25$  nsec which is much shorter than the reciprocal of the  $4722\text{\AA}$  spontaneous transition probability. We concluded after examination of the transition probability data, that the best value for the  $4722\text{\AA}$  bismuth line is  $5.3 \times 10^6 \text{ sec}^{-1}$ . Too slow a risetime of the excitation pulse therefore cannot be the explanation. Based on the WTB measurements for 40eV electrons, an unfavorable ratio of electron cross sections for excitation of the upper resonance and lower metastable levels also does not appear to be the explanation.

A computer model was constructed to examine the laser kinetics and assess the effect of competing processes within the bismuth atom. When rates based on the transition probabilities of Corliss and Bozman are used, the computer model predicts a population inversion and laser action. Further examination indicates that the Corliss-Bozman value for the  $6p^2 7s^4 P_{3/2} \rightarrow 6p^3 4S_{3/2}$  competing resonance transition appears to be at least 20 times too low. A substantial increase in this rate could prevent the establishment of a population inversion. Additional computer modeling studies should be carried out to complete this analysis. The resulting conclusions may also be important in the analysis of efficient pulsed laser action in other atomic vapor systems.

## 15. REFERENCES

1. W. T. Walter, N. Solimene, M. Piltch and G. Gould, "Efficient Pulsed Gas Discharge Lasers," IEEE J. Quantum Electron. QE-2, 474 (1966).
2. G. R. Fowles and W. T. Silfvast, "High-Gain Laser Transition in Lead Vapor," Appl. Phys. Lett. 6, 236 (1965).
3. M. Piltch, W. T. Walter, N. Solimene, G. Gould and W. R. Bennett, Jr., "Pulsed Laser Transitions in Manganese Vapor," Appl. Phys. Lett. 7, 309 (1965).
4. W. T. Walter, M. Piltch, N. Solimene and G. Gould, "Pulsed-Laser Action in Atomic Copper Vapor," Bull. Am. Phys. Soc. 11, 113 (1966).
5. W. T. Walter, "Metal Vapor Lasers," IEEE J. Quantum Electron. QE-4, 355 (1968).
6. J. S. Deech and J. H. Sanders, "New Self-Terminating Laser Transitions in Calcium and Strontium," IEEE J. Quantum Electron. QE-4, 474 (1968).
7. P. Cahuzac, "Raies Laser Infrarouges dans les Vapeurs de Terres Rares et d'Alcalino-Terreux," J. Phys. (Paris) 32, 499 (1971).
8. A. A. Isaev, M. A. Kazaryan and G. G. Petrash, "Effective Pulsed Copper-Vapor Laser with High Average Generation Power," [JETP Lett. 16, 27 (1972)] ZhETF Pis. Red. 16, 40 (1972).
9. D. Alpert, A. O. McCoubrey and T. Holstein, "Imprisonment of Resonance Radiation in Mercury Vapor," Phys. Rev. 76, 1257 (1949). A factor of  $\tau$  is missing from the formula given in footnote 7 of this reference.
10. C. H. Corliss and W. R. Bozman, Experimental Transition Probabilities for Spectral Lines of Seventy Elements, "Nat'l. Bur. Stand. Monograph No. 53 (U.S. Government Printing Office, Washington, D. C., 1962).
11. W. F. Meggers, C. H. Corliss and B. F. Scribner, "Tables of Spectral Line Intensities," Nat'l. Bur. Stand. Monograph No. 32 (U.S. Govt. Printing Office, Washington, D. C., 1961).
12. B. V. Lvov, "Determination of the Absolute Values of Oscillator Strengths by Combined Measurement of the Total and Linear Absorption of Vapor Layers in a Graphite Cell," Optics and Spectroscopy 19, 282 (1965).
13. P. A. Rice and D. V. Ragone, "Simultaneous Determination of  $f$  Values and Vapor Pressures from Optical Absorption Measurements," J. Chem Phys. 42, 701 (1965).
14. P. T. Cunningham and J. K. Link, "Measurement of Lifetimes of Excited States of Na, Tl, In, Ga, Cu, Ag, Pb and Bi by the Phase-Shift Method," J. Opt. Soc. Am. 57, 1000 (1967).

15. S. Svanberg, thesis, University of Gothenburg, May 1972 as quoted in Ref. 16.
16. T. Andersen, O. H. Madsen and G. Sørensen, "Radiative Lifetimes in Sn I and Bi I," J. Opt. Soc. Am. 62, 1118(1972).
17. L. Holmgren, "Theoretically Calculated Transition Probabilities and Lifetimes for the First Excited Configuration  $np^2(n+1)s$  in the Neutral As, Sb and Bi Atoms," Physica Scripta 11, 15(1975).
18. M. D. Kunisz and J. Migdalek, "Theoretical Values of Certain Transitions of Type  $6p^3-6p^27s$  in the Bismuth Atomic Spectrum in Intermediate Coupling," Acta Physica Polonica A47, 231(1975).
19. A. N. Nesmeyanov, "Vapor Pressure of the Chemical Elements," edited by R. Gary (Elsevier, Amsterdam, Netherlands, 1963).
20. R. Hultgren, R. L. Orr, P. D. Anderson and K. K. Kelley, "Selected Values of Thermodynamic Properties of Metals and Alloys," (John Wiley and Sons, New York, 1963).
21. D. R. Stull and G. C. Sinke, "Thermodynamic Properties of the Elements," (Advances in Chemistry Series No. 18, American Chemical Society, Washington, D. C., 1956).
22. Alfred Leu, "Untersuchungen an Wismut nach der magnetischen Molekularstrahlmethode," Zeitschrift für Physik 49, 498 (1928).
23. I. F. Zartman, "A Direct Measurement of Molecular Velocities," Phys. Rev. 37, 383 (1931).
24. Cheng Chuan Ko, "The Heat of Dissociation of  $Bi_2$  determined by the Method of Molecular Beams," J. Franklin Institute 217, 173(1934).
25. M. Yosiyama, J. Chem. Soc. Japan 62, 204(1941). The values used in this report were those quoted in Table 252, page 303 of Reference 19 above.
26. A. T. Aldred and J. N. Pratt, "Vapor Pressure of Liquid Bismuth," J. Chem. Phys. 38, 1085 (1963).
27. J. H. Kim and A. Cosgarea, Jr., "Study of the Vapors of Liquid Lead and Bismuth," J. Chem. Phys. 44, 806(1966).
28. A. K. Fischer, "Vapor Pressure of Bismuth," J. Chem. Phys. 45, 375(1966).
29. F. J. Kohl, O. M. Uy and K. D. Carlson, "Cross Sections for Electron-Impact Fragmentation and Dissociation Energies of the Dimer and Tetramer of Bismuth," J. Chem. Phys. 47, 2667(1967).

30. L. Rovner, A. Drowart and J. Drowart, "Mass Spectrometric Determination of Dissociation Energies of Molecules Bi<sub>2</sub>, Bi<sub>3</sub>, Bi<sub>4</sub> and BiPb," Trans. Faraday Society 63, 2906 (1967).
31. H. E. J. Schins, R. W. M. van Wijk and B. Dorpema, "The Heat-Pipe Boiling-Point Method and the Vapor Pressure of Twelve Metallic Elements in the Range 10-10<sup>4</sup> Torr," Zeitschrift für Metallkunde 62, 330(1971).
32. D. R. Stull and H. Prophet, "JANAF Thermochemical Tables," Second Edition, Nat. Stand. Ref. Data Ser., Nat. Bur. Stand. (U.S.), 37 (U.S. Govt. Printing Office, Washington, D. C., June 1971).
33. G. M. Almy and F. M. Sparks, "The Absorption Spectrum of Diatomic Bismuth," Phys. Rev. 44, 365 (1933).
34. G. Gerber and H. P. Broida, "Electronic States and Molecular Constants of Bi<sub>2</sub>," J. Chem. Phys. 64, 3423 (1976).
35. W. T. Walter, N. Solimene, J. T. LaTourrette and K. Park, "Chemically-Generated Copper Vapor Lasers," Polytechnic Institute of N. Y. Progress Report No. 38 to JSTAC (Polytechnic Institute of N. Y., Report No. R-452-38-73, Nov. 1973).
36. C. J. Chen, N. M. Nerheim and G. R. Russell, "Double-discharge copper vapor laser with copper chloride as a lasant," Appl. Phys. Lett. 23, 514(1973).
37. C. E. Moore, "Atomic Energy Levels," National Bureau of Standards Circular 467 Vol. 3 (U.S. Government Printing Office, Washington, D. C. (1958).
38. W. Williams, S. Trajmar and D. G. Bozinis, "Elastic and Inelastic Scattering of 40eV electrons from Atomic and Molecular Bismuth," J. Phys. B: Atom. Molec. Phys. 8, L96-9 (1975).
39. W. Williams and S. Trajmar, "Elastic and Inelastic Electron Scattering at 20 and 60eV from Atomic Cu," Phys. Rev. Lett. 33, 187 (1974).
40. W. Williams and S. Trajmar, "Elastic and inelastic electron scattering of 40eV electrons from atomic lead," J. Phys. B: Atom. Molec. Phys. 8, L50 (1975).
41. D. Trainor, A. Mandl and H. Hyman, "Metal Vapor Visible Laser Kinetics Program," Report No. AD-A022 596/1WH by AVCO Everett Research Laboratory to ARPA (February 1976).
42. D. A. Leonard, "A Theoretical Description of the 5106-Å Pulsed Copper Vapor Laser," IEEE J. Quantum Electron. QE-3, 380 (1967).
43. E. U. Condon and G. H. Shortley, "The Theory of Atomic Spectra," (Cambridge University Press (1967).



## APPENDIX I

### IMPROVED VALUES OF ATOMIC TRANSITION PROBABILITIES

W. T. Walter and N. Solimene

The rate at which an appropriately excited atom or molecule spontaneously radiates in a particular spectral line is characterized by a transition probability,  $A_{ul}(\text{sec}^{-1})$ , which is sometimes referred to as the Einstein A coefficient. The wavelength of the spectral line is related to the energies of the upper (u) and lower (l) levels,  $\lambda = hc/(E_u - E_l)$ . Accurate values of these transition probabilities are required whenever the kinetics of processes involving excited states of atoms or molecules are examined; for example, in the search for more efficient visible and ultraviolet lasers, in the study of chemical reactions, for astrophysical determinations of solar abundances, interstellar cloud composition, etc.

Transition probabilities can be both calculated and measured. They can be calculated from first principles only for the lightest elements, but the calculations may be extended to heavier elements by including experimental parameters. Experimental measurements of transition probabilities can be divided into two classes; (1) methods which require knowledge of the density of the radiating species, such as the hook method of Rozhdestvenskii and emission and absorption techniques, and (2) methods which are independent of the vapor density such as level crossing, optical double resonance and phase shift techniques. Only these latter measurement methods can be relied upon to give values with an absolute accuracy approaching 10%. Beam foil spectroscopy can be included with these more accurate methods if one can be certain that there is no unrecognized cascading from higher levels.

Although recent work has produced more accurate values of some spectral lines in selected elements, the work of Corliss and Bozman<sup>1</sup> remains the broadest treatment of transition probabilities presently available. Corliss and Bozman used the spectral line intensities measured by Meggers, Corliss and Scribner<sup>2</sup> to calculate transition probabilities of some 25,000 classified lines in 70 elements. Meggers, Corliss and Scribner had measured the peak intensities, I, of 39,000 spectral lines radiated from free-burning 10A dc arcs in air between electrodes of copper to which 1 atom in 1000 of the element of interest had been added. Unfortunately when the Corliss and Bozman values are compared with the more accurate values determined by density-independent methods, errors as large as a factor of 20 have been found. There is therefore a widespread reluctance to use the Corliss and Bozman values, although in many cases they are the only ones available.

Because the Corliss and Bozman values remain the only consistent set of transition probabilities spanning the stronger spectral lines of most of the solid elements, there has been considerable interest in attempting to improve these values. Three

## APPENDIX I

types of corrections have been suggested: an energy dependent correction, an intensity dependent correction and a correction in the copper arc temperature. Huber and Tobey<sup>3</sup> and subsequently others have shown that the energy-dependent normalization function which Corliss and Bozman applied should in fact be a constant. Although originally Corliss and Bozman took the copper arc temperature to be 5100°K, Corliss<sup>4</sup> subsequently suggested that the temperature may actually be as high as 7000°K. Others have suggested temperature corrections. Most recently Degenkolb and Griffiths<sup>5</sup> suggested 6000°K on the basis of comparison with more accurate transition probabilities for the three elements Mg, Ca and Al.

In the Meggers-Corliss-Scribner arc only one atom in 1000 belongs to the element of interest; the rest are copper. When 0.1 atomic percent of the copper atoms are replaced by an element whose ionization potential<sup>6</sup> (IP) is close to or above that of copper (IP = 7.724 eV), the physical properties of the discharge, such as the electron distribution and temperature, should not be appreciably changed. On the other hand if the ionization potential of the added element is substantially lower than that of copper, then a noticeably lowering of the electron and arc temperatures could be observed.

For an optically thin gas, one in which effects due to self-absorption can be neglected, the intensity of the light spontaneously emitted in a particular spectral line  $\lambda$  due to  $N_u$  atoms in the upper energy level is

$$I = N_u A_{ul} hc/\lambda \quad (1)$$

If the gas is in local thermodynamic equilibrium so that the population of the emitting atomic species can be characterized by a Boltzmann distribution, then

$$\frac{N_u}{g_u} = \frac{N_o}{g_o} e^{-E_u/kT} \quad (2)$$

where the  $g$ 's represent the statistical weights of the ground (o) and upper (u) energy levels.

Now in terms of the partition function

$$U = \sum_{u=0}^{\text{all levels}} g_u e^{-E_u/kT} \quad (3)$$

and the total number of the emitting atomic species

$$N = \sum_{u=0}^{\text{all levels}} N_u = \frac{N_o}{g_o} N \quad (4)$$

## APPENDIX I

we can express

$$\ln \frac{I\lambda^3}{gf} = C - \frac{1}{kT} E_u \quad (5)$$

where

$$C = \frac{8\pi^2 e^2 h}{m} \frac{N}{U} \quad (6)$$

is a constant for each light-emitting species. Here the Ladenburg oscillator strength,  $f$ , has been used instead of the transition probability,  $A_{ul}$ . The relationship is

$$gf = g_l f_{lu} = g_u f_{ul} = \frac{mc\lambda^2}{8\pi^2 e^2} g_u A_{ul} = 1.499\lambda^2 g_u A_{ul} \quad (7)$$

If transition probabilities or  $f$  values are available for an element from one of the density-independent methods, the presence of a straight line plot of  $\log (I\lambda^3/gf)$  versus  $E_u$  indicates that the arc can be characterized by a Boltzmann distribution. The arc temperature can then be determined from the slope of the line. When we carried out a linear least squares analysis on such plots for elements with ionization potentials within 1 eV of that of copper, we found Boltzmann temperatures of approximately 6200°K as indicated in Table I.

In fact we find that if we take account of the different values<sup>10</sup> for the atomic partition functions by plotting

$$\ln \frac{I\lambda^3}{gf} U = C_1 - \frac{1}{kT} E_u \quad (7)$$

where  $C_1 = CU = \frac{8\pi^2 e^2 h}{m} N$ , then the points for all 129 spectral lines listed in Table I, together with those for 2 Ag spectral lines<sup>11</sup> (IP = 7.574eV) and 3 Pb spectral lines<sup>12</sup> (IP = 7.415eV) can be very satisfactorily fitted by a single Boltzmann temperature of 6230°K as shown in Figure 1. The fact that the intercept  $C_1$  is the same for different elements indicates that the numbers of emitting atoms are the same. This corroborates Corliss and Bozman's claim that the copper electrodes diluted 1 atom in 1000 with the element of interest dispense atoms of each element into the arc at the same rate. Furthermore it indicates that demixing effects which would tend to reduce the concentration of lighter elements and those with ionization potential substantially below that of copper are not important for the elements we have examined.

Contrary to the claim of Degenkolb and Griffiths,<sup>5</sup> Ca and Al do not yield similar temperatures. The arc temperature does appear to decrease as the ionization potential of the added element in the Meggers-Corliss-Scribner copper arc is lowered

# APPENDIX I

TABLE I. Meggers-Corliss-Scribner Arc temperatures determined from least squares analyses of the slopes of plots of  $\log(I\lambda^3/gf)$  versus  $E_u$ .

Element	Ionization Potential <sup>6</sup>	Number of Spectral Lines	Ref. for f or $A_{ul}$ Values	Arc Temperature
Fe	7.87 eV	85	7	6121°K
Cu	7.724eV	6	4 and 8	6395°K
Mg	7.644eV	19	9	6235°K
Ti	6.82 eV	19	7	6285°K

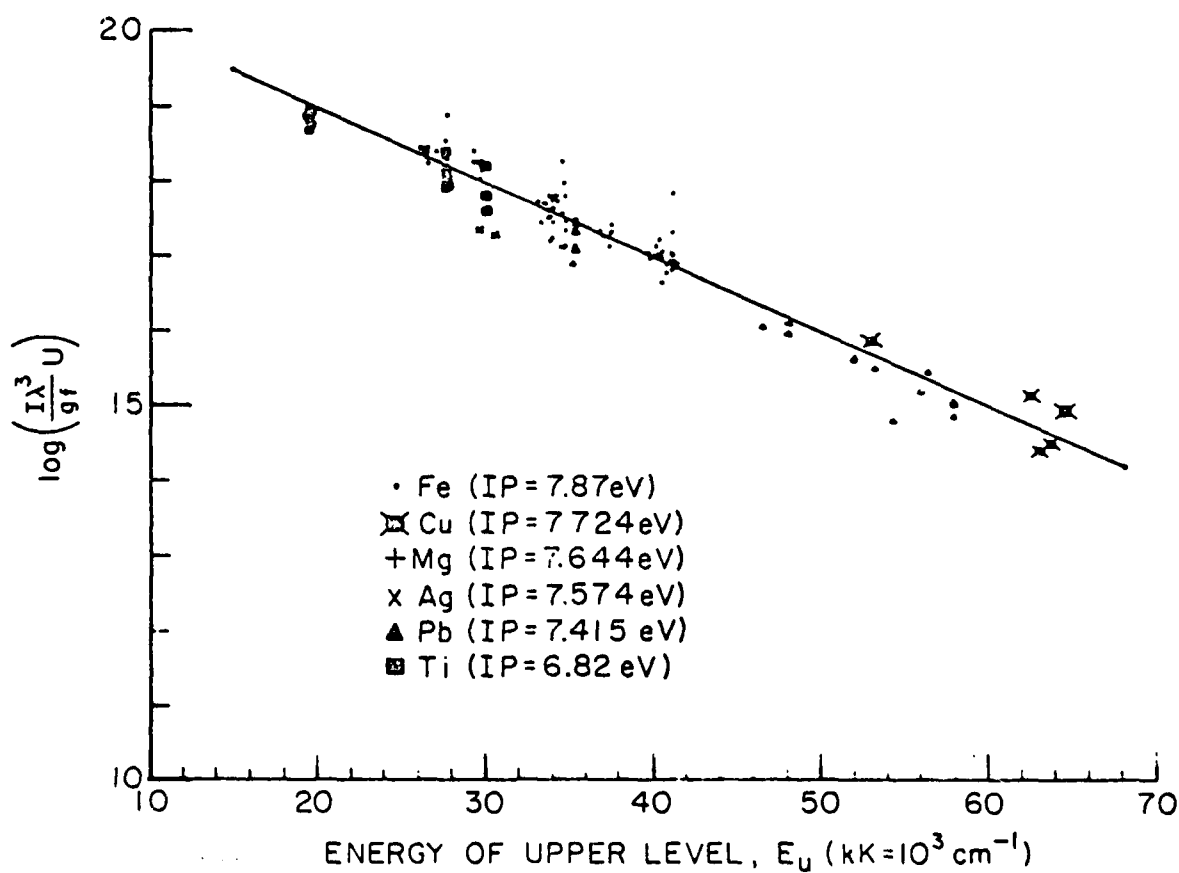


Fig. 1. Semilog plot of intensities of 134 spectral lines from 6 elements with ionization potentials within 1 eV of that of copper. The straight line least squares fit indicates a Boltzmann distribution at 6230°K for the Meggers-Corliss-Scribner arc.

## APPENDIX I

more than approximately 1 eV below that of copper. For example the temperature we determined for 65 spectral lines of Ca (IP = 6.11 eV) was 5037°K and for 12 spectral lines of Al (IP = 5.984 eV) was 5441°K.

Therefore we suggest that for the 52 elements in the Corliss and Bozman tables with ionization potentials > 6.8 eV, the temperature of the Meggers-Corliss-Scribner arc should be taken as 6230°K. In addition use of the partition function for each element will superimpose the spectral lines of all of these elements on a single Boltzmann-distribution linear semilog plot. Improved transition probabilities can then be obtained without having a single absolute transition probability measured within that element. Work is continuing at the Polytechnic to determine the range of validity of this procedure as well as to determine the increase in accuracy.

Joint Services Technical Advisory Committee  
F44620-74-C-0056

W.T. Walter and N. Solimene

ARPA under Office of Naval Research Contract  
N00014-67-A-0438-0017

Office of Naval Research  
N00014-67-A-0438-0015

## REFERENCES

1. C. H. Corliss and W. R. Bozman, "Experimental Transition Probabilities for Spectral Lines of Seventy Elements," National Bureau of Standards Monograph 53 (Washington, D. C.: U. S. Government Printing Office, 1962).
2. W. F. Meggers, C. H. Corliss and B. F. Scribner, "Tables of Spectral-Line Intensities," National Bureau of Standards Monograph 32 (Washington, D. C.: U. S. Government Printing Office, 1961). Intensities, I, taken from Ref. 2 have been multiplied by 1000 to compensate for the 0.1 atomic percentage dilution in the arc.
3. M. Huber and F. L. Tobey, "gf-Values of Ultraviolet Fe I, Cr I and Cr II Lines from Shock-Tube Measurements," *Astrophys. J.* 152, 609 (1968).
4. C. H. Corliss, "A Review of Oscillator Strengths for Lines of Cu I," *J. Res. Nat. Bur. Stand. (U. S.)*, 74A, 781 (1970).
5. E. O. Degenkolb and J. E. Griffiths, "Temperature of the Meggers-Corliss-Scribner Copper Arc," *J. Opt. Soc. Am.* 65, 315 (1975).
6. Ionization potentials have been taken from Table 34, page xxxiv of C. E. Moore, "Atomic Energy Levels," National Bureau of Standards Circular 467 Vol. 3 (Washington, D. C.: U. S. Government Printing Office, 1958).
7. D. C. Morton and W. H. Smith, "A Summary of Transition Probabilities for Atomic Absorption Lines Formed in Low-Density Clouds," *Astrophys. J. Suppl.* 26, 333 (1973).
8. C. H. Corliss, "Spectral-Line Intensities and gf-Values in the First Spectrum of Copper," *J. Res. Nat. Bur. Stand. (U. S.)*, 66A, 497 (1962). The intensities, I, of 6 spectral lines of Cu taken from Ref. 8 (4248, 4480, 4509, 4539, 4586 and 4704 Å) were used directly and not multiplied by 1000 to account for dilution. Accurate transition probabilities have been determined by Kock and Richter<sup>4</sup> for these 6 lines which were too weak to be observed in the arc between diluted electrodes<sup>2</sup> but were observed in an arc between pure copper electrodes.<sup>8</sup> For this reason the transition probabilities of these 6 lines should be weak enough that their intensities, I, were not affected by self-absorption in a pure copper arc.

## APPENDIX I

9. W. L. Wiese, M. W. Smith and B. M. Miles, "Atomic Transition Probabilities II - Sodium through Calcium," National Bureau of Standards Monograph NSRDS-NBS 22 (Washington, D. C.: U. S. Government Printing Office, 1969).
10. H. W. Drawin and P. Felenbok, "Data for Plasmas in Local Thermodynamic Equilibrium," (Paris: Gauthier-Villars, 1965).
11. P. T. Cunningham and J. K. Link, "Measurement of Lifetimes of Excited States of Na, Tl, In, Ga, Cu, Ag, Pb and Bi by the Phase-Shift Method," J. Opt. Soc. Am. 57, 1000 (1967).
12. E. B. Saloman and W. Happer, "Lifetime, Coherence Narrowing and Hyperfine Structure of the  $(6s^2 6p 7s) 3P_1^o$  State in Lead," Phys. Rev. 144, 7 (1966).

## APPENDIX II

### COMPUTER MODELING OF THE DYNAMICS OF METAL VAPOR LASERS

N. Solimene and W. T. Walter

The experimental investigation of metal vapor lasers, in particular the copper vapor laser,<sup>1</sup> and the search for new metal vapor lasers<sup>2</sup> are significant parts of the laser work at the institute. For this reason it was felt that numerical modeling of the dynamics of such lasers would be a useful adjunct to the experimental effort. Consequently a start in the development of a computer model has been made.

#### A. The Model

The model includes rate equations for the populations of various energy levels which are directly or indirectly involved in the development of actual or potential laser action. Also included are rate equations for the populations of additional atomic species which may be present to act as buffer gases or to facilitate electrical breakdown and discharge. The primary excitation is provided by electron collisions. De-excitation may be by electron collisions, as well as by other mechanisms such as radiative relaxation and diffusion to walls and subsequent de-excitation. The rate constants for transitions between the various energy levels and for ionization depend on the cross sections for these processes and on the electron number density and energy distribution. To simplify the model, the electron energy distribution is assumed to have a known functional form throughout the discharge pulse, but the average electron energy is permitted to change in a manner determined by an energy balance equation. Convenient distributions are the Maxwell-Boltzmann and the Druyvesteyn distribution.

## APPENDIX II

This type of model has been used by Gerry<sup>3</sup> to investigate the pulsed molecular nitrogen laser, and by Leonard<sup>4</sup> to investigate the copper vapor laser.

Since in most cases the cross sections for ionization or for excitation are not known, they have been estimated using the semiclassical formulas of Gryzinski.<sup>5</sup> The specific rate constants are then calculated as a function of electron temperature in the Boltzmann case, or as a function of the average electron energy in the Druyvesteyn case.

The circuit equations for capacitor voltage and discharge current density are those used by Gerry and Leonard. The ohmic resistance term depends on the momentum transfer cross sections for the various species and the electron energy distribution. It is believed that the correct treatment of this term will be of some importance in correlating experimental results involving different buffer species. This will require, however, good estimates of the momentum transfer cross sections. For the present, ad hoc estimates are being used. It is hoped that classical phase shift calculations will provide better estimates which will be incorporated later on.

The ohmic resistance also enters in an ohmic heating term in the energy balance equation for the average electron energy. Other terms are energy transfer terms which describe excitation, de-excitation, and ionization. The electron number density is determined by the ionization rates for the atomic species present and by electron loss terms such as recombination. The latter are being ignored for the present since they are expected to be important only in the after-glow when the laser action is completed.

Phenomenological equations for the laser photon densities are included for each of the potential laser transitions. Output power densities may be computed using effective optical cavity time constants.

### B. The Equations

#### 1. Circuit Equations

$$\frac{dV}{dt} = -\frac{A}{C} j$$

$$\frac{dj}{dt} = \frac{1}{LA} (V - \rho \ell j),$$

where



## APPENDIX II

$V$  = voltage across capacitor  
 $j$  = current density  
 $C$  = capacitance  
 $L$  = circuit inductance  
 $l$  = length of discharge  
 $A$  = cross-sectional area of discharge  
 $\rho$  = discharge resistivity.

Note that  $\rho$  depends on electron energy distribution.

### 2. Electron Equations

$$\frac{dN_e}{dt} = N_e \sum_k \sum_i N_i^{(k)} R_i^{(k)},$$

$$\begin{aligned} \frac{d}{dt} (N_e \epsilon_0) = & \rho j^2 - N_e \sum_k \sum_i N_i^{(k)} R_i^{(k)} (E^{(k)} - E_i^{(k)}) \\ & - N_e \sum_k \sum_{i,j} N_i^{(k)} R_{ij}^{(k)} (E_i^{(k)} - E_j^{(k)}), \end{aligned}$$

where

$N_e$  = electron number density

$\epsilon_0$  = average electron energy

$N_i^{(k)}$  = atom number density of  $k^{\text{th}}$  component in  $i^{\text{th}}$  energy level

$E^{(k)}$  = ionization energy for  $k^{\text{th}}$  species

$E_i^{(k)}$  = energy of  $i^{\text{th}}$  level for  $k^{\text{th}}$  component

$R_i^{(k)}$  = specific electron ionization rate for  $k^{\text{th}}$  component in  $i^{\text{th}}$  energy level

$R_{ij}^{(k)}$  = specific electron excitation (de-excitation) rate from  $i^{\text{th}}$  to  $j^{\text{th}}$  level of  $k^{\text{th}}$  species.

Note that  $R_i^{(k)}$  and  $R_{ij}^{(k)}$  depend on electron energy distribution in a manner which is detailed below.

### 3. Population Equations

## APPENDIX II

$$\begin{aligned}
 \frac{dN_i^{(k)}}{dt} = & -N_e N_i^{(k)} R_i^{(k)} + N_e \sum_j \left( N_j^{(k)} R_{ji}^{(k)} - N_i^{(k)} R_{ij}^{(k)} \right) \\
 & + \sum_j \left\{ \left( N_j^{(k)} - N_{j,eq}^{(k)} \right) \left( \frac{1}{\tau_{ji}^{(k)}} + A_{ji}^{(k)} \right) - \left( N_i^{(k)} - N_{i,eq}^{(k)} \right) \left( \frac{1}{\tau_{ij}^{(k)}} + A_{ij}^{(k)} \right) \right\} \\
 & + \delta_{k,1} \sum_n \delta(n,i) B_n \left( N_{n(2)}^{(1)} - \frac{g_{n(2)}}{g_{n(1)}} N_{n(1)}^{(1)} \right) P_n, \\
 & k = 1, 2, \dots, c, \quad i = 1, 2, \dots, s(k);
 \end{aligned}$$

where

- $c$  = number of components in gas mixture
- $s(k)$  = number of energy levels for  $k^{\text{th}}$  component
- $N_{i,eq}^{(k)}$  = equilibrium number density at gas temperature
- $\tau_{ij}^{(k)}$  = relaxation time for  $i^{\text{th}}$  to  $j^{\text{th}}$  level of  $k^{\text{th}}$  component due to gas or wall collisions
- $A_{ij}^{(k)}$  = spontaneous emission coefficient
- $n(2)$  = index for upper level of  $n^{\text{th}}$  laser transition
- $N_{n(2)}^{(1)}$  = number density in upper level of  $n^{\text{th}}$  laser transition
- $n(1)$  = index for lower level of  $n^{\text{th}}$  laser transition
- $g_j$  = degeneracy of  $j^{\text{th}}$  energy level in  $1^{\text{st}}$  component
- $\delta(n,i) = \begin{cases} +1 & \text{if } i = n(1) \\ -1 & \text{if } i = n(2) \\ 0 & \text{otherwise} \end{cases}$
- $B_n$  = stimulated emission coefficient for  $n^{\text{th}}$  laser transition
- $P_n$  = photon density for  $n^{\text{th}}$  laser transition.

### 4. Laser Photon Density Equations

$$\begin{aligned}
 \frac{dP_n}{dt} = & -\frac{1}{\tau_n} P_n + B_n \left( N_{n(2)}^{(1)} - \frac{g_{n(2)}}{g_{n(1)}} N_{n(1)}^{(1)} \right) P_n + \frac{B_n N_{n(2)}^{(1)}}{V_n} \\
 & n = 1, 2, \dots, n_L
 \end{aligned}$$

## APPENDIX II

where

$n_l$  = number of laser transitions

$\tau_n$  = relaxation time for  $n^{\text{th}}$  laser transition

$V_n$  = effective mode volume .

### 5. Specific Rate Constants

$$R_i^{(k)} = \int_0^{\infty} \sigma_i^{(k)}(\epsilon) \sqrt{\frac{2\epsilon}{m}} f(\epsilon, \epsilon_0) d\epsilon$$

$$R_{ij}^{(k)} = \int_0^{\infty} \sigma_{ij}^{(k)}(\epsilon) \sqrt{\frac{2\epsilon}{m}} f(\epsilon, \epsilon_0) d\epsilon ,$$

where

$\sigma_i^{(k)}(\epsilon)$  = cross section for electron ionization of  $i^{\text{th}}$  energy level in  $k^{\text{th}}$  component as function of electron energy

$\sigma_{ij}^{(k)}(\epsilon)$  = cross section for electron excitation (de-excitation) from  $i^{\text{th}}$  to  $j^{\text{th}}$  energy level in  $k^{\text{th}}$  component as function of electron energy

$m$  = electron mass

$f(\epsilon, \epsilon_0)$  = electron energy distribution function with average energy equal to  $\epsilon_0$ .

#### a. Maxwell-Boltzmann Distribution

$$f(\epsilon, \epsilon_0) = \frac{2}{kT_e} \sqrt{\frac{\epsilon}{\pi kT_e}} e^{-\epsilon/kT_e}$$

$$\begin{cases} \epsilon_0 = \frac{3}{2} kT_e \\ T_e = \text{electron temperatures} \end{cases} .$$

#### b. Druyvesteyn Distribution

$$f(\epsilon, \epsilon_0) = \frac{2}{\epsilon_0 \Gamma(3/4)} \sqrt{\frac{\epsilon}{\epsilon_0}} e^{-0.55(\epsilon/\epsilon_0)^2}$$

### 6. Discharge Resistivity

## APPENDIX II

$$\rho = \frac{3}{2} \frac{m}{e^2 N_e} \sum_k N^{(k)} R^{(k)}$$

$$R^{(k)} = \int_0^{\infty} \sigma^{(k)}(\epsilon) \sqrt{\frac{2\epsilon}{m}} f(\epsilon, \epsilon_0) d\epsilon ,$$

where:

$e$  = electron charge

$N^{(k)}$  = total number density of  $k^{\text{th}}$  component

$\sigma^{(k)}(\epsilon)$  = momentum transfer cross section for electron collisions with  $k^{\text{th}}$  species as function of electron energy.

### C. Numerical Procedure and Results

The above system of nonlinear differential equations which results from the model is integrated using the HPCCG routine in the Fortran SSP library.

The routine was, however, modified so that the step size is controlled by the relative error rather than absolute error. The reason for this is the large dynamic range of the variables involved, as well as their disparate magnitudes. Also, the allowed number of step-size halvings was increased in order to get past the gas-breakdown phase of the time development.

Some preliminary results have been obtained using a prototypic three-level copper energy level structure with no buffer species. These results are reasonable in terms of known experimental behavior, but will not be described, since their only purpose was to aid the program development. It is hoped that this model can be sufficiently well developed so that it will be capable of not only correlating experimental data but also of guiding future experiments in copper, bismuth and other metals.

Joint Services Technical Advisory Committee  
F44620-69-C-0047

N. Solimene

### REFERENCES

1. W. T. Walter, N. Solimene, J. T. LaTourrette, and K. Park, "Chemically-Generated Copper Vapor Lasers," Progress Report No. 38 to JSTAC, Polytech. Inst. of New York, Report No. R-452.38-73 (1973).
2. K. Park, N. Solimene, and W. T. Walter, "Investigation of Cyclic Laser Action in Bismuth Vapor," Progress Report No. 38 to JSTAC, Polytech. Inst. of New York, Report No. R-452.38-73 (1973).

## APPENDIX II

3. E. T. Gerry, "Pulsed-Molecular-Nitrogen Laser Theory," Appl. Phys. Letters, 7, 6-8 (1965).
4. D. A. Leonard, "A Theoretical Description of the 5106-<sup>0</sup>Å Pulsed Copper Vapor Laser," IEEE J. Quantum Electron., QE-3, 380-81 (1967).
5. M. Gryzinski, "Classical Theory of Atomic Collisions. I. Theory of Inelastic Collisions," Phys. Rev., 138A, 336-58 (1965); also, A. E. S. Green, "Electron Impact Cross Sections for Aeronomy," AIAA J., 4, 769-75 (1966).